

Model-Twin Randomization (MoTR): A Monte Carlo Method for Estimating the Within-Individual Average Treatment Effect Using Wearable Sensors

Eric J. Daza, DrPH, MPS (Evidation, Stats-of-1)

Logan Schneider, MD (Stanford Medicine, Alphabet)

August 3, 2022

Please send correspondence to: Eric J. Daza (ericdaza@statsof1.org)

Abstract

Temporally dense single-person “small data” have become widely available thanks to mobile apps and wearable sensors. Many caregivers and self-trackers want to use these data to help a specific person change their behavior to achieve desired health outcomes. Ideally, this involves discerning possible causes from correlations using that person’s own observational time series data. In this paper, we estimate within-individual average treatment effects of physical activity on sleep duration, and vice-versa. We introduce the model twin randomization (MoTR; “motor”) method for analyzing an individual’s intensive longitudinal data. Formally, MoTR is an application of the g-formula (i.e., standardization, back-door adjustment) under serial interference. It estimates stable recurring effects, as is done in n-of-1 trials and single case experimental designs. We compare our approach to standard methods (with possible confounding) to show how to use causal inference to make better personalized recommendations for health behavior change, and analyze 222 days of Fitbit sleep and steps data for one of the authors.

Keywords: causal inference, n-of-1, time series, longitudinal, digital, wearable, personalized

1 Introduction

The ever-increasing abundance of frequently collected, temporally dense single-person *small data* [1, 2] has fueled the desire to extract “personalized insights” from this digital individual-level information. However, standard analyses of such *intensive longitudinal data* [3] merely characterize statistical associations, making conclusions of causal effects generally hard to defend.

Causal effects are needed to make these insights truly “actionable” to the extent that one actually expects to see an impact from intervening on a measured factor. Epidemiologists and econometricians have developed and used causal inference methods to better inform population-level policies and decisions to improve societal outcomes. How can behavior change scientists likewise apply these methods to within-individual observational studies—in order to better inform individual-level behavioral interventions and habit-changing practices?

One solution is to conduct within-individual experiments via the mobile phone apps and wearable or implantable sensors that enable small-data collection. These could be simple randomized or forced crossover designs as are commonly used in within-individual studies (see below), that do not generally require causal inference methods.

Individuals with common recurring or chronic health conditions in particular could benefit from such digitally informed “self-experiments”. These conditions include migraines, chronic pain, asthma, and irritable bowel syndrome [ref]. However, substantial barriers to self-experimentation exist for these conditions [ref], highlighting the need to make better use of dense digital data by extracting insights that are not just “correlational” (i.e., statistically associated) but also plausibly causal.

1.1 Within-Individual Studies

An n-of-1 trial is a randomized single-person crossover trial [4]; i.e., one individual undergoes multiple crossover periods with varying treatments [5, 6]. The target population in an n-of-1 trial is the largely unobserved superset of periods experienced by one person. Specifically, it is the set of all possible time periods wherein the subject is at risk for the chronic health condition, and is under at least one of the treatment conditions being studied both during and outside of the n-of-1 trial total study period (i.e., before and after all n-of-1 treatment periods, in the “real world”). Hence, we can speak of this target population as a “population of yourself” or “population-of-1”.

Biomedical research and clinical trials in particular have successfully employed n-of-1 trials [7, 8, 9, 10, 11, 12], with trial design, implementation, and analysis guidance available in various texts [5, 13, 14, 15, 16]. Chen et al (2012) [17] argued that wearable sensors can be used to facilitate n-of-1 trials. And both a recent article in Nature [18] and the U.S. Department of Health and Human Services Agency for Healthcare Research and Quality (AHRQ) [5] have considered n-of-1 trials to be part of “personalized medicine”.

Single-case experimental designs (SCEDs) in psychology and n-of-1 trials in clinical settings are experimental single-person crossover studies focused on, though not always limited to, one individual. These two types of studies differ in design, but both are used to infer average individual-specific outcomes under different intervention levels. Each average is taken across a set of consecutive (though not necessarily contiguous) time intervals with the same exposure level. These intervals are called *phases* in SCEDs, and *periods* in n-of-1 trials.

Both SCEDs and n-of-1 trials share the same underlying statistical foundations and target estimands. In statistics, quantities that describe or apply to repeated measures taken on one study participant are described as “within-subject” or “within-individual”. (Examples include the within-subject sum-of-squares, within-cluster variance, and the intra-cluster or intraclass correlation in mixed- or random-effects models and survey sampling.) Hence, we will collectively call SCEDs, n-of-1 trials, and their observational (i.e., non-experimental/non-randomized) counterparts “within-individual” studies, similar to “idiographic” studies in psychology [19].

Contrast these with hierarchical or multilevel models, which are used in group-level or “nomothetic” studies to infer an average outcome taken across a set of repeatedly measured individuals. Their target population consists of a largely unobserved superset of individuals. For example, Araujo et al (2016) [20] provide a good exposition on the relationship between n-of-1 trials and mixed-effects models. In the special case of a longitudinal study, longitudinal models are used to posit and infer a population-average trend taken

across a set of individual trends. We elaborate on the relationship between within-individual studies and hierarchical models (and Bayesian inference) in the Appendix.

1.2 Within-Individual Causal Inference

We define a single-person crossover observational study to be a non-experimental, non-randomized study of one person, wherein recurring confounding and selection bias may exist. Our particular single-person crossover observational study objective is to discover plausible causal effects of would-be interventions that could be tested in a subsequent single-person crossover experiment like an n-of-1 trial or SCED.

Using the Neyman-Rubin-Holland counterfactual framework [21, 22, 23] as a scientific foundation, Daza (2018) [24] formalized a single-person crossover observational study analytical framework for inferring a single-person crossover average treatment effect (ATE). He called this within-individual ATE the *average period treatment effect* (APTE), based on the n-of-1 trial “period”. The APTE can be thought of as a recurring average individual treatment effect.

The APTE framework elaborates on the implicit causal assumptions underlying the dynamic regression models of Vieira et al (2017) [25], specified for a single individual from the original formulation in Schmid (2001) [26] and Kravitz et al (2014) [5]. It additionally enables a counterfactual interpretation of repeated effects over n-of-1 trial periods or SCED phases by stating common analytic challenges in terms of potential outcomes, including outcome autocorrelation and time trends (over multiple periods), and intervention carryover effects.

Daza demonstrated the utility of the APTE framework by applying two common causal inference methods, the g-formula (a.k.a., standardization, back-door or regression adjustment) and propensity-score inverse probability weighting, to infer a possible average effect of his physical activity on his weight. He used health activity data self-tracked over a six-year period. Balandat (2016) [27] took a similar approach towards causal prediction of electricity consumption using a prognostic-score technique [28], and developed the large-sample theory needed to conduct inference on the APTE if exposure effects do not carry over from one period to the next.

Cheung et al (2017) [29] set the stage for comparing nomothetic and idiographic modeling of the APTE using tree-based approaches. Burg et al (2017) [30] accomplished a similar goal through mixed-effects modeling using generalized linear models. Balandat also drew a formal connection between individual- and group-level average treatment effects in his Section 4.5.

In this paper, we propose a Monte Carlo method called model-twin randomization (MoTR, pronounced “motor”) for estimating the APTE. This approach involves first modeling the outcome as a function of all causes, and then running this “model twin” through a simulated n-of-1 trial by randomizing the exposure at each time point to generate an effect estimate. MoTR is an application of the theory in both Daza (2018) [24] and the design-based approach of Wang (2021) [31].

1.3 Why Study Sleep?

The timing of sleep and wake is believed to be regulated by 2 main underlying processes: the homeostatic drive and the circadian rhythm [32]. The homeostatic drive is a use-state negative feedback process that accumulates over periods of wakefulness and dissipates over periods of sleep. The circadian rhythm is an intrinsic set of biological oscillations with approximately 24-hour (i.e., “circa” means about; “diem” means day) periodicity.

Each of these biological processes are regulated by not only the primary sleep period, but also by an organism’s behaviors throughout the waking period. From the standpoint of the sleep homeostasis, the primary somnogen, adenosine, is a breakdown product of the energy molecule adenosine triphosphate (ATP), indicating that it is not just the amount of preceding wakefulness, but the intensity of that wakefulness (i.e., highly active vs sedentary) that dictates the subsequent sleep drive.

Similarly, there are a number of environmental exposures and biological processes (cumulatively termed zeitgebers or “time givers”) that help synchronize the body’s intrinsic biorhythms to meet the organismal needs. Most of these signals—from dietary intake to light level and color variation—are integrated via a “master clock” in the hypothalamus to orchestrate the molecular clocks present in every other cell of the body.

The aforementioned physiologic processes help to regulate the intrinsic sleep-wake state neurocircuitry in order to meet the needs of the organism (e.g., keeping nocturnal animals up at night). However, there is a wide range of variation in how these processes play out, even within species. Genome-wide association studies (GWAS) in humans have discovered polygenic contributions to the wide range of variation in typical sleep duration/need [33] and intrinsic circadian phase (i.e., “chronotype” [34]).

However, it seems that the intrinsic organismal needs also reflect the function that sleep serves in maintaining health. For example, families of individuals with mutations conferring short sleep need seem to sleep more effectively than others, as is evidenced by their physiologic and functional resilience to very short sleep durations [35, 36]. Studies of transgenic mice showing less neurodegeneration in response to chronic sleep restriction provide further evidence [37]. Taken together, there seems to be not only a genetically determined setpoint for sleep need and timing, but also an individual-specific resilience to perturbations of the sleep-wake system.

The current gold-standards of sleep physiologic measurements are quite impractical: from the resource-intensive and disruptive nature of sleeping in a research laboratory to gather neurophysiologic, cardiopulmonary, and behavioral signals, to the highly controlled environment and inconvenient sampling requirements needed to isolate true circadian biomarker measurements (e.g., dim-light melatonin onset). On the other end of the spectrum, affording more real-world convenience at scale, self-report sleep and circadian measures—such as the Morningness-Eveningness questionnaire [38], Munich Chronotype Questionnaire [39], and the Consensus Sleep Diary [40]—are plagued with recall bias and inaccuracy [41]. Toward this end, technologies that are able to gather sufficiently accurate data offer a unique opportunity for exploring the interrelationship between sleep and wake.

It is important to note that what is gained in convenience comes at the expense of what is lost in fidelity. For example, sleep-tracking technologies that depend on non-electroencephalographic signals don’t accurately recapitulate in-lab polysomnograms [42, 43]. That being said, such sensors perform reasonably well in their general estimation of the daily amounts of sleep and wake [44], particularly in the generally healthy populations on which their algorithms were trained.

Similarly, different activity trackers have varying accuracy, depending upon context [45]. However, despite the known limitations in accuracy in how wearables measure both sleep and wake activities, their consistency in measurement longitudinally is core to the potential value they bring to understanding the impact of deliberate interventions or unintended changes within an individual.

For these reasons, examining sleep and how it relates to other behavioral metrics as measured by wearable sensors is an ideal target application for the development of idiographic causal inference methods. For example, one can examine varying the exposure to factors that impact the physiologic sleep drive to infer the APTE of that factor on sleep. Chevance et al (2021) [46] examined such associations, but stopped short of attempting to draw causal inferences. A reasonable treatment phase or period could be one day, given that periods of sleep, by their very nature, tend to “wash out” the effect of increased sleep pressure resulting from increased levels of waking activity. The target estimand of interest would be the true APTE of the exposure (e.g., activity level) on that particular night’s sleep quantity; i.e., the average effect taken over all days throughout the individual’s life.

1.4 Paper Structure

The rest of this paper is organized as follows. In Section 2, we define key notation and causal inference concepts. We introduce the autoregressive carryover model for estimating an APTE that is stable in the long run. We then introduce MoTR as a Monte Carlo (numerical) method for estimating the APTE in Section 3, and demonstrate its performance through a simulation study in Section 4. In Section 5, we use MoTR (and a complementary propensity-score method) to estimate the APTE of sleep duration on steps per minute using 222 days of EJD’s Fitbit Charge 3 data. We conclude in Section 6 with a short summary, and propose future directions. All analyses were conducted in R version 3.6.3.

2 Methodological Theory

2.1 Notation, Definitions, and Assumptions

Throughout this article, we define a *data-generating function or mechanism* (or simply *mechanism*) as the true, unknown equation that relates input variables or predictors to an outcome variable. We define a *model* as a statistical equation that is fit to data, which may or may not approximate the true DGF. This distinction reflects the famous Box aphorism that “all models are wrong, but some are useful”. Our notation is as follows.

Random variables and fixed values are written in upper-case and lower-case, respectively. Let $p(A = a)$ denote the probability mass or density of random variable A at a , with shorthand $p(a)$. For any random variable B , let $B|A$ denote the relationship “ B conditional on A ”, with shorthand $B|a$ for $B|A = a$. Let $B \perp\!\!\!\perp A$ denote statistical independence of B and A . Let $E(\cdot)$ denote the expectation function, and let $I(\cdot)$ denote the identity function such that $I(b) = 1$ if expression b is true and $I(b) = 0$ otherwise.

We will use the following set notation. Let $\{a\}$ denote a set with elements $\{a_1, a_2, \dots\}$. Likewise, let \mathbf{a} denote a vector with elements denoted with commas as in (a_1, a_2, \dots) , or without commas as in $(a_1 a_2 \dots)$. Assume all vectors multiplied together are conformable; e.g., a $1 \times p$ random vector \mathbf{A} and its $p \times 1$ coefficient vector $\boldsymbol{\beta}_A$ can be vector-multiplied as $\mathbf{A}\boldsymbol{\beta}_A$.

Let $(\{A_t\}) = (A_1, A_2, \dots)$ denote a stochastic process or time series (i.e., vector of ordered random variables or vectors). For any non-empty set S , let $\{\mathbf{a}\}$ denote the set of all permutations of all possible values of the vector \mathbf{a} , not including the empty set \emptyset .

2.2 Causal Inference

Let Y represent a variable occurring after a binary variable X with support $s \in \{0, 1\}$. If $E(Y|X = 0) \neq E(Y|X = 1)$ when X is randomized, then we say there is a *direct effect* of X on Y , and that X is a *direct cause* of Y . Let \mathbf{W} represent the set of all other direct or indirect causes of Y that may also be direct or indirect causes of X , or may *contextualize* (i.e., modify or moderate) the effect of X on Y .

An indirect cause affects the outcome through other mediating factors, forming a causal path from the indirect cause to the outcome through the *mediators*. Causes of both X and Y *confound* causal interpretations of the statistical dependence between X and Y , and hence are called *confounders*. An effect contextualizer is not directly manipulable, but the effect of X on Y varies across the contexts it represents (e.g., day of week).

The observable outcome Y can then be written as a function of X , \mathbf{W} , and completely random error \mathcal{E} (e.g., due to random between-measurement variation). Let $Y = g(X, \mathbf{W}, \mathcal{E})$ represent this *structural causal mechanism* (i.e., true “structural causal model” that generates the data); for example, $g(X, \mathbf{W}, \mathcal{E}) = \beta_0 + \beta_1 X + \mathbf{W}\boldsymbol{\beta}_2 + \mathcal{E}$.

Now let Y^s denote the value of Y corresponding to s . This is the outcome that would be observed whenever $X = s$, and hence is called the *potential outcome* (PO) of an exposure variable X . For $x \in \{0, 1\}$, the relevant potential outcomes are Y^1 and Y^0 . The potential outcome Y^s can then be written as a function of \mathbf{W} and \mathcal{E} . Let $Y^s = g_s(\mathbf{W}, \mathcal{E})$ represent this PO mechanism. In design-based or randomization-based causal inference, the randomness in Y is assumed to result only from the assignment of X to 1 or 0; hence, the POs are treated as fixed values (implying \mathbf{W} is also treated as fixed), and so are written simply as y^1 and y^0 .

The observed outcome Y , intervention of interest X , and potential outcomes $\{Y^s\}$ are related by the equivalence $Y = \sum_{\{s\}} Y^s I(X = s)$, with shorthand $Y = Y^X$. This equivalence is called *causal consistency*, and simply states that the observed outcome is equal to its corresponding PO. (We will refer to statistical consistency, the asymptotic unbiasedness of an estimator, simply as “consistency”.) Recalling our earlier example, because $x \in \{0, 1\}$, we have $Y = Y^1 X + Y^0(1 - X)$. Under causal consistency, one natural set of PO mechanisms is $Y^1 = \beta_0 + \beta_1 + \mathbf{W}\boldsymbol{\beta}_2 + \mathcal{E}$ and $Y^0 = \beta_0 + \mathbf{W}\boldsymbol{\beta}_2 + \mathcal{E}$. The randomization-based counterpart to this model-based or superpopulation-based approach involves the same equations, but with fixed \mathbf{w} and ε .

Causal consistency formalizes the *fundamental problem of causal inference* [23] that the only observable PO is the one corresponding to $X = s$. Hence, the term *counterfactual outcome* (or simply *counterfac-*

tual) is often used to refer to $Y^{x'}$ for $x' \neq x$. “Counterfactuals” and “potential outcomes” are often used synonymously.

Statistical causal inference commonly involves four conditions. When the POs occur independently of X , the assignment mechanism is said to be ignorable, and that *ignorability* or unconfoundedness holds [47, 48]. We will see that this condition is implied under randomization; i.e., $\{Y^s\} \perp\!\!\!\perp X$ if X is randomized. If the POs occur independently of X given all other causes \mathbf{W} , then *conditional ignorability* holds; i.e., $\{Y^s\} \perp\!\!\!\perp X | \mathbf{W}$ [49].

The third condition, called *positivity* or *overlap*, is the empirical requirement that all elements in the support of X must necessarily co-occur with all other causes. For example, if $w \in \{0, 1\}$, then positivity holds if there is at least one observation for each unique pair of \mathbf{w} and x . That is, positivity holds if each element of $\{(w, x)\} = \{(0, 0), (0, 1), (1, 0), (1, 1)\}$ is observed in the data. Positivity is required for estimating the average treatment effect, defined in Section 2.4.

The fourth condition that must hold is the stable unit treatment value assumption (SUTVA) [50]. A key component of this condition is that the POs of a given individual are not affected by any other individual’s treatment assignment. That is, there is no *interference* between individuals [51, 52]. Formally, let $\{Y_i^1, Y_i^0\}$ and $\{Y_{i'}^1, Y_{i'}^0\}$ denote the PO sets of distinct individuals i and i' , respectively.

If interference exists, then individual i instead has POs $\{Y_i^{11}, Y_i^{10}, Y_i^{01}, Y_i^{00}\}$, where $Y_i^{s_i s_{i'}}$ denotes the potential outcome if individual i receives treatment s_i while individual i' receives treatment $s_{i'}$. Likewise holds for individual i' . Causal consistency in this case is defined as $Y = \sum_{\{s_i, s_{i'}\}} Y^{s_i s_{i'}} I(X_i = s_i, X_{i'} = s_{i'})$, with shorthand $Y = Y^{X_i X_{i'}}$. These studies require careful characterization, selection, and estimation of the relevant estimand [53]. We will see that autocorrelation and treatment carryover from past periods generate serial interference in single-person crossover studies; i.e., what Wang, 2021[31], calls “temporal interference”.

A fifth condition that is often overlooked but is important for establishing effect transportability (i.e., generalization of a treatment effect to a non-experimental setting) is called *distributional stability* [54, 55, 56, 57] or *invariance* [58]. Invariance holds if the distribution of the outcome conditional on some subset of predictors does not change across all possible environments or intervention regimes (e.g., randomized vs. observed). [24] called the special case wherein randomization status neither affects the outcome nor is affected by any confounders *randomization invariance*.

If randomization invariance holds, then randomization status is an instrumental variable that satisfies the exclusion restriction. That is, randomization status is associated with the exposure, but not with any confounders, the outcome, or variation in the outcome not explained by the exposure or confounders. Neto et al (2016, 2017) [59, 60] exploited this property of randomization to try to estimate single-person crossover personalized average causal effects.

2.3 Why Use Potential Outcomes?

The PO framework is generally not needed to conduct causal inference in simple or straightforward cases. From our example, we could just evaluate the model $Y = \beta_0 + \beta_1 X + \mathbf{W} \beta_2 + \mathcal{E}$ directly when X is randomized. So why use it?

The power of the PO framework, elaborated in Section 2.4, is in handling the complexity of commonplace cases that have become particularly ubiquitous in the era of data science. These span both observational studies with their non-randomized predictors (e.g., convenience samples, real-world data, health claims, medical records, user behavior) and experimental studies with their randomized interventions (e.g., A/B testing, experimentation, network effects, etc.).

Thinking in terms of POs also implicates methods of statistical inference that are far from obvious when one is mainly concerned with how to statistically predict or model an outcome—the main focus of modern data science and machine learning. For example, the PO framework allows causal inference to be understood as a missing data or survey sampling problem, or to be conducted via randomization-based inference (in contrast to the superpopulation-based inference central to statistical modeling and machine learning). This key insight is the reason we now have propensity score matching and inverse probability weighting (IPW) methods [47]. POs also encourage development, implementation, and detailed characterization and analysis of discrete interventions that are intuitive and actionable (e.g., “do A=1 or A=0”).

2.4 Average Treatment Effect

In a nomothetic study, participant $i \in \{1, \dots, n\}$ with $\mathbf{W}_i = \mathbf{w}$ and $\mathcal{E}_i = \varepsilon$ is thought to have a set of fixed POs $\{y_i^s\}$ with the same number of elements as $\{s\}$, as in design-based or randomization-based causal inference. That is, individual i has the two fixed POs y_i^1 and y_i^0 , and a difference between y_i^1 and y_i^0 is called an *individual treatment effect* (ITE).

The superpopulation-based counterparts to this randomization-based definition involve the same quantities, but with random \mathbf{W} and \mathcal{E} , yielding random POs Y_i^1 and Y_i^0 . Here, the randomness in Y is additionally assumed to result from other mechanisms such as random sampling of study participants, or random variation over time (even just throughout the study period). We will see in Section 2.5 onward that our time-series-based setting requires us to assume that at least some confounders are realizations of randomly varying quantities. Hence, we will expound on the superpopulation-based approach here to set up the theory for Section 2.5.

While of primary interest, the ITE is not identifiable due to the fundamental problem of causal inference. However, if X is randomized for all individuals, then $E(Y^s)$ (i.e., the mean PO taken across all individuals) is identifiable using only observed data because

$$\begin{aligned} E(Y|X = x) &= E(Y^X|X = x) \text{ by causal consistency} \\ &= E(Y^x|X = x) \\ &= E(Y^x) \text{ if } X \text{ is randomized.} \end{aligned} \tag{1}$$

A difference between $E(Y^1)$ and $E(Y^0)$ is called an *average treatment effect* (ATE). Here, the expectations are taken over all study participants. In randomization-based causal inference, $E(Y^s)$ is taken across all study participants with unchanging confounders, contextualizers, and errors. In the superpopulation-based framework, $E(Y^s)$ is taken across the superpopulation consisting of all possible realizations of each study participant (i.e., the supports of \mathbf{W}_i and \mathcal{E}_i) for all participants.

Recall the example in Section 2.1 with $Y_i^1 = \beta_0 + \beta_1 + \mathbf{W}_i\beta_2 + \mathcal{E}_i$ and $Y_i^0 = \beta_0 + \mathbf{W}_i\beta_2 + \mathcal{E}_i$. First, note that the ITE specified as $Y_i^1 - Y_i^0$ is equal to β_1 , regardless of individual. This is an important and common assumption in nomothetic causal inference when there is no interference: The ITEs are all equal to the same constant quantity, even though each potential outcome may be random. In general, we will assume that the ITE is a constant for each individual, as it is here. To indicate that this is a fixed quantity that is nonetheless comprised of random components, we will denote this using the lowercase $\delta_i^{\text{ITE}} = Y_i^1 - Y_i^0$.

In this example, the ATE specified as $\delta^{\text{ATE}} = E(\delta^{\text{ITE}}) = E(Y^1 - Y^0) = E(Y^1) - E(Y^0)$ is also constant and equal to β_1 . This expectation is taken over all individuals, who all have $\delta_i^{\text{ITE}} = \beta_1$, *when X is randomized for all individuals*. Hence, the ITEs are all equal to the ATE.

An ATE that varies based on some elements of \mathbf{W} is called a conditional ATE (CATE) for heterogeneous treatment effects; i.e., the ATE is heterogenous across subgroups defined by values or levels of \mathbf{W} . The CATE is a more realistic estimand in many cases, and we will estimate an idiographic type of CATE using real data in Section 5.

The ATE is the primary estimand of interest in a randomized study like a randomized controlled trial (RCT) or A/B test because all other causes \mathbf{W} need not be observed in order to estimate the difference between $E(Y^1)$ and $E(Y^0)$. That is, if X is randomized for (i.e., randomly assigned to) each individual, then estimates of $E(Y|X = s)$ —instead of $E(Y^s)$ —can be used to estimate the ATE without needing to observe \mathbf{W} or know how it functionally relates to Y . This result conveys the power of randomization as a tool for elucidating causal mechanisms. The key assumption, as shown in our example above, is that the ITEs are all identical.

In an observational study, it does not generally follow that $E(Y|X = x) = E(Y^x)$. This is because \mathbf{W} may also affect X . When X is not randomized, equation (1) only holds true up to $E(Y|X = x) = E(Y^x|X = x)$. Hence, estimates of $E(Y|X = 1)$ and $E(Y|X = 0)$ cannot be used to estimate the ATE. The effect of \mathbf{W} on X *confounds* straightforward estimation of the ATE, so \mathbf{W} is called a *confounder*. If all confounders are observed, standard approaches to estimating the ATE from observational data can be used. We describe two of these in Section 3.

2.5 Average Period Treatment Effect

In an idiographic study, a single participant i is measured repeatedly over phases or periods $t \in \{1, \dots, m\}$. For now, we will drop the i index because we will only address one participant.

Let Y_t represent a recurring variable occurring after a recurring binary variable X_t . Let \mathbf{W}_t represent the set of all other causes of Y_t that may also be causes of X_t . The individual at period t with $\mathbf{W}_t = \mathbf{w}$ and $\mathcal{E}_t = \varepsilon$ is thought to have a set of fixed POs y_t^1 and y_t^0 . Following Daza (2018) [24], we will call the ITE analogue in this setting a *period treatment effect* (PTE), defined as a difference between y_t^1 and y_t^0 . As mentioned earlier, we will develop our theory around the PTE superpopulation-based counterparts Y_t^1 and Y_t^0 .

The PTE is not identifiable due to the fundamental problem of causal inference. However, if X is randomized at every period, then $E(Y^s)$ (i.e., the mean PO taken across all periods) is identifiable using only observed data by the analogous derivation to (1). In this time series setting, we will invoke the sequential analogues of ignorability and conditional ignorability.

A difference between $E(Y^1)$ and $E(Y^0)$ is called an *average period treatment effect* [24]. In this paper, we will take this average over the superpopulation comprised of all observed periods $1, \dots, m$. In the future, a broader goal that reflects those of nomothetic causal generalizability or transportability might be to estimate an APTE taken over all possible relevant periods throughout the participant’s life (e.g., the times when they are at risk for condition Y at varying levels of exposure X).

Let us modify our earlier example of PO mechanisms from Section 2.1 as $Y_t^1 = \beta_0 + \beta_1 + \mathbf{W}_t\beta_2 + \mathcal{E}_t$ and $Y_t^0 = \beta_0 + \mathbf{W}_t\beta_2 + \mathcal{E}_t$. Like with our original example, note that the PTE specified as $\delta_t^{\text{PTE}} = Y_t^1 - Y_t^0$ is equal to β_1 regardless of period. In general, we will assume that the PTE is a constant at each period, as it is here. As with the analogous ATE from earlier, the APTE specified as $\delta^{\text{APTE}} = E(\delta^{\text{PTE}})$ is also constant and equal to β_1 , where the expectation is taken over all periods *when X is randomized at every period*.

This example reflects the common assumption in n-of-1 trials that the PTEs are all equal to the same constant quantity regardless of period. We will call this property *effect constancy*; i.e., $\delta_t^{\text{PTE}} = \beta_1$ in our example. This follows because all associations between the predictors X_t and \mathbf{W}_t and the observed outcome $Y_t = \beta_0 + \beta_1 X_t + \mathbf{W}_t\beta_2 + \mathcal{E}_t$ are constant; i.e., the coefficients don’t depend on t . Daza (2018) described such a predictor-specific association as being *stable* [24]. This is a property of n-of-1 trials with no serial interference across periods due to, for example, autocorrelation and carryover of the treatment’s influence from past periods (see Sections 2.7 and 2.8).

The APTE is the primary estimand of interest in an n-of-1 trial because all other recurring causes \mathbf{W} need not be observed in order to estimate the difference between $E(Y^1)$ and $E(Y^0)$. That is, if X is randomized at each period (as in a standard n-of-1 trial), then estimates of $E(Y|X = s)$ —instead of $E(Y^s)$ —can be used to estimate the APTE without needing to observe \mathbf{W} or know how it functionally relates to Y . The key assumption, as shown in our modified example, is that the PTEs are all identical when there is no serial interference.

However, we cannot generally ignore or mitigate autocorrelation and carryover in observational (i.e., non-experimental) real-world digital health settings. We will need to allow for serial interference across periods. Hence, while we will assume that the PTE is constant at each period, we will not assume that the PTEs are all equal to a single APTE.

2.6 N-of-1 Objective

Our overall research goal is to answer the behavior-change self-tracking question, “What is a possible sustained effect (i.e., APTE) of X on Y , that I might be able to modify?” For example, “What is a possible average effect of taking more than my average number of steps per minute on my sleep duration if I keep this up over a week, versus taking fewer than my average number of steps per minute during that same week?” Here, we say an APTE is *sustained* once it ceases to change after repeated assignment of the same treatment level over successive periods. This is the between-period equivalent of within-period *effect stability* described in Daza (2018) [24].

Autocorrelation and carryover can delay an APTE from becoming sustained, and addressing these phenomena in order to answer our initial question is out of scope for this paper. Instead, we will first lay the groundwork by answering the easier question, “What is the APTE of X on Y if we were to randomize X at every period under similar conditions?” This can be answered by expanding the typical n-of-1 trial approach

to allow autocorrelation and carryover to influence the APTE. Hence, we will describe such a study wherein X is randomized at every period as an n -of-1 *experiment* to distinguish it from the standard constraints enforced in an n -of-1 trial.

2.7 Temporal Considerations

Relationships between variables across periods complicate estimation and interpretability of an APTE in ways not commonly encountered in estimating an ATE—even when interference is present. These complications arise from autocorrelation, time trends, carryover, and slow onset or decay [5].

Autocorrelation occurs if Y_t depends on its history up to ℓ^Y lagged outcomes $\bar{Y}_t^{\ell^Y} = (L, L^2, \dots, L^{\ell^Y})Y_t$, where L^k is the lag operator defined as $L^k Y_t = Y_{t-k}$. Note that Y_t need not depend on all lags up to ℓ^Y . For example, Y_t could depend on \bar{Y}_t^4 only through (L^1, L^3, L^4) or (L^2, L^4) for a given mechanism.

Let $\mathbf{V}_t \in \mathbf{W}_t$ denote the set of exogenous causes of Y_t , such that \mathbf{V}_t is never itself affected by X or Y . For example, a temporal cycle like weekday, week of month, month, annual quarter, or season could be included in \mathbf{V}_t . If all lagged outcomes in $\bar{Y}_t^{\ell^Y}$ affect Y_t , then the structural causal mechanism is $Y_t = g(X_t, \bar{Y}_t^{\ell^Y}, \mathbf{V}_t, \mathcal{E}_t)$. For simplicity of exposition, we will assume that there are no endogenous causes of Y_t (i.e., that are affected by Y , and maybe X) from here until Section 2.10; i.e., that $\mathbf{V}_t = \mathbf{W}_t$.

For example, suppose $Y_t = \beta_0 + \beta_X X_t + \beta_{ar} Y_{t-1} + \mathbf{V}_t \beta_{ex} + \mathcal{E}_t$, where AR stands for “autoregressive” (see Section 2.10). For all such examples of linear models, we will assume $|\beta_{ar}| < 1$ for all lagged outcome coefficients; this is called the *stationarity condition* in econometrics [61]. We will also assume that $\{\mathbf{V}_t\}$ is jointly covariance stationary; equivalently, that joint weak- or wide-sense stationarity (WSS) holds. These two conditions imply that $\{Y_t\}$ is WSS, ensuring our initial assumption is met.

A *time trend* is defined as a sequential trend in the outcomes over successive periods such that $E(Y_t)$ increases or decreases across periods, rendering $\{Y_t\}$ no longer WSS. For example, the mean outcome $E(Y_t)$ increases with t as with $Y_t = \beta_0 + \beta_X X_t + \beta_{trend} t + \mathbf{V}_t \beta_{ex} + \mathcal{E}_t$ where $\beta_{trend} > 0$.

Carryover is defined as “the tendency for treatment effects to linger beyond the crossover (when one treatment is stopped and the next one started)” [5]. Suppose Y_t depends on some set of lagged treatments $\bar{X}_t^{\ell^X} = (L, L^2, \dots, L^{\ell^X})X_t$. If all lagged treatments in $\bar{X}_t^{\ell^X}$ affect Y_t , then the structural causal mechanism is $Y_t = g(X_t, \bar{X}_t^{\ell^X}, \mathbf{V}_t, \mathcal{E}_t)$. In such cases, we say that carryover, carryover influence, or treatment carryover exists.

2.8 Serial Interference and Effect Modification

The presence of carryover or autocorrelation means that the POs at a given period are influenced by treatment assignment in past periods. That is, carryover can create *serial interference* over time, as noted in the randomization-based temporal approaches of Wang (2021) [31] and Aronow and Samii (2013) [62]. Notably, we will see in the following example that carryover does not necessarily modify the PTE itself.

If carryover is present, recall that the structural causal mechanism is $Y_t = g(X_t, \bar{X}_t^{\ell^X}, \mathbf{V}_t, \mathcal{E}_t)$. To illustrate, suppose $\bar{X}_t^{\ell^X} = X_{t-1}$ and $Y_t = \beta_0 + \beta_X X_t + \beta_{co} X_{t-1} + \mathbf{V}_t + \mathcal{E}_t$ where $\beta_{co} = 0$ at $t = 1$. Let $Y^{s_t s_{t-1}}$ denote the potential outcome if the participant receives treatment s_t at period t , and treatment s_{t-1} at period $t - 1$. The PO mechanism is just $g_{s_t s_{t-1}}(\mathbf{V}_t, \mathcal{E}_t) = \beta_0 + \beta_X s_t + \beta_{co} s_{t-1} + \mathbf{V}_t + \mathcal{E}_t$. Serial interference exists, and the POs at period t are $\{Y_t^{11}, Y_t^{10}, Y_t^{01}, Y_t^{00}\}$. *Serial causal consistency* states that $Y_t = Y_t^{X_t X_{t-1}} = \sum_{\{s_t, s_{t-1}\}} Y_t^{s_t s_{t-1}} I(X_t = s_t, X_{t-1} = s_{t-1})$.

We will follow the approach Hudgens and Halloran (2008) [53] took in defining the “individual average PO”. Let $Y_t^{s_t^*}$ denote the *contemporaneous average PO* (CAPO) at period t corresponding to s_t . This is the potential outcome at period t under treatment level s at that same period, averaged over all possible treatment level combinations over all past periods; in this case, just $s_{t-1} \in \{0, 1\}$. That is, $Y_t^{s_t^*} = E_{X_{t-1}}(Y^{s_t X_{t-1}} | X_t = s_t) = Y_t^{s_t 1} \Pr(X_{t-1} = 1 | X_t = s_t) + Y_t^{s_t 0} \Pr(X_{t-1} = 0 | X_t = s_t)$.

Similarly, let $Y_t^{*s_{t-1}}$ denote the *carryover average PO* at period t corresponding to s_{t-1} . This is the potential outcome at period t under treatment level s at the previous period, $t - 1$, averaged over all possible treatment level combinations in the current period; in this case, just $s_t \in \{0, 1\}$. That is, $Y_t^{*s_{t-1}} = E_{X_t}(Y^{X_t s_{t-1}} | X_{t-1} = s_{t-1}) = Y_t^{1 s_{t-1}} \Pr(X_t = 1 | X_{t-1} = s_{t-1}) + Y_t^{0 s_{t-1}} \Pr(X_t = 0 | X_{t-1} = s_{t-1})$.

Table 1: Carryover example: No effect modification.

$Y_t^{s_t s_{t-1}}$	$\beta_0 + \beta_X s_t + \beta_{co} s_{t-1} + \mathbf{V}_t + \mathcal{E}_t$
Y_t^{11}	$\beta_0 + \beta_X + \beta_{co} + \mathbf{V}_t + \mathcal{E}_t$
Y_t^{10}	$\beta_0 + \beta_X + \mathbf{V}_t + \mathcal{E}_t$
Y_t^{01}	$\beta_0 + \beta_{co} + \mathbf{V}_t + \mathcal{E}_t$
Y_t^{00}	$\beta_0 + \mathbf{V}_t + \mathcal{E}_t$

Table 2: Carryover example: Effect modification.

$Y_t^{s_t s_{t-1}}$	$\beta_0 + \beta_X s_t + \beta_{co} s_{t-1} + \beta_{Xco} s_t s_{t-1} + \mathbf{V}_t + \mathcal{E}_t$
Y_t^{11}	$\beta_0 + \beta_X + \beta_{co} + \beta_{Xco} + \mathbf{V}_t + \mathcal{E}_t$
Y_t^{10}	$\beta_0 + \beta_X + \mathbf{V}_t + \mathcal{E}_t$
Y_t^{01}	$\beta_0 + \beta_{co} + \mathbf{V}_t + \mathcal{E}_t$
Y_t^{00}	$\beta_0 + \mathbf{V}_t + \mathcal{E}_t$

We now redefine the PTE as a difference between the CAPOs $Y_t^{1\bullet}$ and $Y_t^{0\bullet}$, which we specify as the difference $\delta_t^{\text{PTE}} = Y_t^{1\bullet} - Y_t^{0\bullet}$. We likewise define the carryover effect as a difference between the carryover average POs $Y_t^{1\bullet}$ and $Y_t^{0\bullet}$, which we specify as the difference $\delta_t^{co} = Y_t^{1\bullet} - Y_t^{0\bullet}$. Adapting the terminology of Hudgens and Halloran (2008) [53], both differences would be *period average direct causal effects*.

Continuing our example, suppose X is randomized to 0 or 1 with equal probability (i.e., all conditional probabilities are equal to 0.5). Table 1 lists the four POs. From this, we see that $Y_t^{1\bullet} = Y_t^{11}0.5 + Y_t^{10}0.5 = \beta_0 + \beta_X + \beta_{co}0.5 + \mathbf{V}_t + \mathcal{E}_t$ and $Y_t^{0\bullet} = Y_t^{01}0.5 + Y_t^{00}0.5 = \beta_0 + \beta_{co}0.5 + \mathbf{V}_t + \mathcal{E}_t$. Hence, we have $\delta_t^{\text{PTE}} = \beta_X$ at any period t . Also note that $Y_t^{1\bullet} = Y_t^{11}0.5 + Y_t^{01}0.5 = \beta_0 + \beta_X0.5 + \beta_{co} + \mathbf{V}_t + \mathcal{E}_t$ and $Y_t^{0\bullet} = Y_t^{10}0.5 + Y_t^{00}0.5 = \beta_0 + \beta_X0.5 + \mathbf{V}_t + \mathcal{E}_t$. Hence, we have $\delta_t^{co} = \beta_{co}$ at any period t . Note that the PTE is β_X regardless of whether or not a carryover effect (and by implication, carryover) exists; i.e., it is β_X both when $\beta_{co} \neq 0$ and $\beta_{co} = 0$. Hence, neither the carryover effect nor influence modifies the PTE.

Now suppose instead that $Y_t = \beta_0 + \beta_X X_t + \beta_{co} X_{t-1} + \beta_{Xco} X_t X_{t-1} + \mathbf{V}_t + \mathcal{E}_t$ where $\beta_{co} = \beta_{Xco} = 0$ at $t = 1$, with the four POs listed in Table 2. We now see that $Y_t^{1\bullet} = \beta_0 + \beta_X + \beta_{co}0.5 + \beta_{Xco}0.5 + \mathbf{V}_t + \mathcal{E}_t$ and $Y_t^{0\bullet} = \beta_0 + \beta_{co}0.5 + \mathbf{V}_t + \mathcal{E}_t$. Hence, $\delta_t^{\text{PTE}} = \beta_X + \beta_{Xco}0.5$ at any period t . The carryover POs are now $Y_t^{1\bullet} = \beta_0 + \beta_X0.5 + \beta_{co} + \beta_{Xco}0.5 + \mathbf{V}_t + \mathcal{E}_t$ and $Y_t^{0\bullet} = \beta_0 + \beta_X0.5 + \mathbf{V}_t + \mathcal{E}_t$. Hence, $\delta_t^{co} = \beta_{co} + \beta_{Xco}0.5$ at any period t . Note that the PTE is just β_X when there is neither a carryover effect nor influence; i.e., $\beta_{co} = -\beta_{Xco}0.5$ and $\beta_{co} = 0$, respectively. However, $\delta_t^{\text{PTE}} = \beta_X - \beta_{co}$ when there is no carryover effect, but there is a carryover influence; i.e., $\beta_{co} = -\beta_{Xco}0.5$, but $\beta_{co} \neq 0$, respectively. That is, carryover modifies the PTE in general—even when there is no carryover effect!

If there is no carryover, autocorrelation can still create serial interference. Recall that the autocorrelation structural causal mechanism is $Y_t = g(X_t, \bar{\mathbf{Y}}_t^{\ell^Y}, \mathbf{V}_t, \mathcal{E}_t)$. For example, suppose $\bar{\mathbf{Y}}_t^{\ell^Y} = Y_{t-1}$, $Y_1 = g(X_1, V_1, \mathcal{E}_1)$, and $Y_t = g(X_t, Y_{t-1}, \mathbf{V}_t, \mathcal{E}_t)$ at $t > 1$. Even in this simple example, the resulting POs undergo a recursive combinatorial expansion with every successive period due to the autocorrelation. Estimating an APTE can easily become intractable with more and more periods.

To see this, note that we are faced with the sequence of PO mechanisms $Y_1^{s_1} = g_{s_1}(V_1, \mathcal{E}_1)$, $Y_2^{s_2 s_1} = g_{s_2 s_1}(Y_1^{s_1} s_1 + Y_1^0(1 - s_1), V_2, \mathcal{E}_2)$, and $Y_3^{s_3 s_2 s_1} = g_{s_3 s_2}(Y_2^{s_2 s_1} s_2 + Y_2^0 s_1(1 - s_2), V_3, \mathcal{E}_3)$. For example, consider our earlier structural causal mechanism $Y_t = \beta_0 + \beta_X X_t + \beta_{ar} Y_{t-1} + \mathbf{V}_t \beta_{ex} + \mathcal{E}_t$ where $\beta_{ar} = 0$ at $t = 1$. Then $Y_1^{s_1} = \beta_0 + \beta_X s_1 + \beta_{ex} V_1 + \mathcal{E}_1$, $Y_2^{s_2 s_1} = \beta_0 + \beta_X s_2 + \beta_{ar} Y_1^{s_1} + \beta_{ex} V_2 + \mathcal{E}_2$, $Y_3^{s_3 s_2 s_1} = \beta_0 + \beta_X s_3 + \beta_{ar} Y_2^{s_2 s_1} + \beta_{ex} V_3 + \mathcal{E}_3$, and so on. We will use this example throughout the rest of this subsection.

2.9 Average Period Effects

Thankfully, the APTE can still be defined in the presence of serial interference. We will first introduce a type of APTE based only on the past exposure history. We will then see how the APTE relates to this

history-based quantity through the CAPO.

Let $\bar{\mathbf{X}}_t \in \{(L, L^2, \dots, L^{t-1})\}$ $X_t = \{(X_{t-1}, X_{t-2}, \dots, X_1)\}$ denote the *full exposure history* wherein X is first assigned at $t = 1$. Following Sävje et al (2021) [63], we define the general formula for the *historical PTE* as $\delta_t(\bar{\mathbf{x}}_t) = Y_t^{1\bar{\mathbf{x}}_t} - Y_t^{0\bar{\mathbf{x}}_t}$. As we did in defining the set of lagged outcomes for autocorrelation, $\bar{\mathbf{X}}_t$ may not contain all past time points. For example, $\bar{\mathbf{x}}_t = x_{t-1}$ at all t in Tables 1 and 2. The historical PTE in Table 1 is always $\delta_t(\bar{\mathbf{x}}_t) = \beta_X$. However, in Table 2 at $t = 1$ we have $\delta_t(\bar{\mathbf{x}}_t) = \beta_X$, while at $t > 1$ we have $\delta_t(1) = \beta_X + \beta_{Xco}$ and $\delta_t(0) = \beta_X$.

We define the corresponding *historical APTE* (HAPTE) as $\delta^{\text{HAPTE}}(\bar{\mathbf{x}}) = \frac{1}{m} \sum_{t=1}^m \delta_t(\bar{\mathbf{x}}_t)$. The HAPTE is the average effect taken over all periods under the observed exposure history up to $m - 1$; i.e., $\bar{\mathbf{x}}_m$. It answers the question, “What was the average effect over my particular history of exposures and unchangeable exogenous characteristics (e.g., weather)?” The HAPTE in Table 1 is always $\delta^{\text{HAPTE}}(\bar{\mathbf{x}}_m) = \frac{1}{m} \sum_{t=1}^m \beta_X = \beta_X$. However, in Table 2 the HAPTE is $\delta^{\text{HAPTE}}(\bar{\mathbf{x}}_m) = \beta_X + I(m > 1) \frac{1}{m} \sum_{t=2}^m I(x_{t-1} = 1) \beta_{Xco}$.

If there is no carryover, autocorrelation, or any other source of serial interference (e.g., an unobserved exogenous confounder V_{t-2} that affects both X_{t-1} and Y_t), then the observed exposure history does not influence the POs. Suppose this is the case, such that there is no serial interference, and therefore $Y_t^{s_t \bar{\mathbf{s}}_t} = Y_t^{s_t}$. Hence, $\delta_t(\bar{\mathbf{x}}_t) = Y_t^1 - Y_t^0$ as would be the case in Table 1 under $\beta_{co} = 0$.

Suppose further that, as in our earlier n-of-1 trial example in Section 2.5, X is randomized at every period, and that the PTEs and APTEs are all equal to the same effect-constant quantity across all periods, denoted δ^{APTE} as before. Then we simply have $\delta^{\text{HAPTE}}(\bar{\mathbf{x}}_m) = \delta^{\text{APTE}}$, so that estimating this trivial APTE is straightforward. (This is also the case in Table 1 because we showed that the HAPTE is constant, implying that its expectation is constant.) This n-of-1 trial answers the question, “What average effect should I have expected at any given period, if I had randomized intervention at that period?”

However, serial interference that produces non-constant HAPTEs (as in Table 2) cannot always be ruled out, and effect constancy will not hold in general, such that $\delta^{\text{HAPTE}}(\bar{\mathbf{x}}_m) \neq \delta^{\text{APTE}}$. To answer n-of-1 questions like the one above, we therefore cannot rely on estimating the HAPTE—even when X is randomized at every period. Instead, we must first generally define each CAPO used to calculate $\delta_t^{\text{PTE}} = Y_t^1 - Y_t^0$.

The general formula for the CAPO resembles the logic of causal consistency. The CAPO is $Y_t^{s_t^*} = Y_t^{s_t}$ at $t = 1$, and otherwise

$$\begin{aligned}
Y_t^{s_t^*} &= E_{\bar{\mathbf{X}}_t} \left(Y_t^{s_t \bar{\mathbf{X}}_t} \mid X_t = s_t \right) \\
&= E_{\bar{\mathbf{X}}_t} \left\{ \sum_{\{\bar{\mathbf{s}}_t\}} Y_t^{s_t \bar{\mathbf{s}}_t} I(\bar{\mathbf{X}}_t = \bar{\mathbf{s}}_t) \mid X_t = s_t \right\} \\
&= \sum_{\{\bar{\mathbf{s}}_t\}} Y_t^{s_t \bar{\mathbf{s}}_t} E_{\bar{\mathbf{X}}_t} \{ I(\bar{\mathbf{X}}_t = \bar{\mathbf{s}}_t) \mid X_t = s_t \} \\
&= \sum_{\{\bar{\mathbf{s}}_t\}} Y_t^{s_t \bar{\mathbf{s}}_t} \sum_{\{\bar{\mathbf{x}}_t\}} I(\bar{\mathbf{X}}_t = \bar{\mathbf{s}}_t) I(\bar{\mathbf{X}}_t = \bar{\mathbf{x}}_t) \Pr(\bar{\mathbf{X}}_t = \bar{\mathbf{x}}_t \mid X_t = s_t) \\
&= \sum_{\{\bar{\mathbf{s}}_t\}} Y_t^{s_t \bar{\mathbf{s}}_t} \Pr(\bar{\mathbf{X}}_t = \bar{\mathbf{s}}_t \mid X_t = s_t). \tag{2}
\end{aligned}$$

Note that δ_t^{PTE} is similar to the “average contemporary direct effect” of Wang (2021) [31]. However, whereas Wang takes the expectation over all individuals at a given period, the expectation in (2) is taken over all periods prior to t for a single individual.

Suppose X is randomized at every period, reducing the conditional probability component of equation (2) to $\prod_{s_k \in \bar{\mathbf{s}}_t} \Pr(X_k = s_k)$, and the CAPO to $Y_t^{s_t^*} = E_{\bar{\mathbf{X}}_t} (Y_t^{s_t \bar{\mathbf{X}}_t})$. Recall our earlier definition that the expectation $E(\delta^{\text{PTE}})$ be taken over all periods when X is randomized at every period in defining δ^{APTE} . Hence, we have

$$\begin{aligned}
\delta^{\text{APTE}} &= E(\delta^{\text{PTE}}) \\
&= \frac{1}{m} \sum_{t=1}^m \delta_t^{\text{PTE}} \\
&= \frac{1}{m} \sum_{t=1}^m (Y_t^{1\cdot} - Y_t^{0\cdot}) \\
&= \frac{1}{m} \sum_{t=1}^m \left\{ E_{\bar{X}_t} \left(Y_t^{1\bar{X}_t} \right) - E_{\bar{X}_t} \left(Y_t^{0\bar{X}_t} \right) \right\} \text{ by randomization of } X_t \\
&= \frac{1}{m} \sum_{t=1}^m \left\{ E_{\bar{X}_t} \left(Y_t^{1\bar{X}_t} - Y_t^{0\bar{X}_t} \right) \right\} \\
&= \frac{1}{m} \sum_{t=1}^m [E_{\bar{X}_t} \{ \delta_t(\bar{X}_t) \}] \\
&= E_{\bar{X}_t} \left\{ \frac{1}{m} \sum_{t=1}^m \delta_t(\bar{X}_t) \right\} \\
&= E_{\bar{X}_m} \{ \delta^{\text{HAPTE}}(\bar{X}_m) \}. \tag{3}
\end{aligned}$$

We see that the APTE is equal to mean HAPTE taken over all possible exposure histories. Sävje et al (2021) [63] call the right side of the second equivalence an *average distributional shift effect*—a generalization of the original group- and population-level quantities in Hudgens and Halloran (2008) [53].

The n-of-1 experimental quantity (3) is our target of inference. It answers the question, “What was the average effect over my particular history of exposures and unchangeable exogenous characteristics, *if I had randomized intervention at every period?*” We can estimate this quantity using only observed data (i.e., without knowing counterfactuals) if X is randomized at every period. To see this, note that the conditional mean observed outcome at a given period is equal to the CAPO.

$$\begin{aligned}
E(Y_t|X_t = x_t) &= E\left(Y_t^{X_t\bar{X}_t}|X_t = x_t\right) \text{ by causal consistency} \\
&= E_{\bar{X}_t}\left(Y_t^{x_t\bar{X}_t}|X_t = x_t\right) \\
&= Y_t^{x_t\cdot} \text{ by (2)} \tag{4}
\end{aligned}$$

Hence, we have $\delta^{\text{APTE}} = \frac{1}{m} \sum_{t=1}^m \{E(Y_t|X_t = 1) - E(Y_t|X_t = 0)\}$ when X is randomized at every period.

Interestingly, note that the APTE of (3) is actually a *conditional APTE* because we do not modify the original values of the unchangeable exogenous characteristics. This reflects how in real life, we would not have been able to modify such characteristics. Specifically, $\delta^{\text{APTE}} = E(\delta^{\text{PTE}}|\mathbf{V}_1, \dots, \mathbf{V}_m)$ where each δ_t^{PTE} only depends on the corresponding \mathbf{V}_t .

Finally, we may be able to estimate an average PO at any period that is stable or constant *in the long run* (i.e., for very long multivariate time series)—and thereby, define and estimate a constant *long-run APTE*—if $\{(\mathbf{W}_t)\}$ is WSS. If such an APTE exists, we will call this property “long-run effect constancy”.

Recall that effect constancy does not require WSS to hold for the average effect to be constant at every period. But effect constancy may be overly optimistic to expect from real-world observational data. In such cases, long-run effect constancy may still be a reasonable property to expect from a large enough sample (i.e., a long-enough multivariate time series). In Section 2.11, we will introduce a model that implies long-run effect constancy.

2.10 Autoregressive Carryover Model

We now define a basic linear model that accounts for both carryover and autocorrelation, that we will call the “autoregressive carryover” (ARCO) model. This model is based on the dynamic regression models of

Vieira et al (2017), Kravitz et al (2014), and Shcmid (2001) [5, 25, 26]. The ARCO model lets us derive some useful long-run averages (including a long-run APTE) under WSS.

We define the ARCO model as

$$Y_t = \beta_0 + \beta_X X_t + \bar{\mathbf{X}}_t^{\ell^X} \boldsymbol{\beta}_{co} + \mathbf{X}_t^{\otimes} \boldsymbol{\beta}_{Xco} + \bar{\mathbf{Y}}_t^{\ell^Y} \boldsymbol{\beta}_{ar} + \mathbf{Y}_t^{\otimes} \boldsymbol{\beta}_{Xar} + \mathbf{V}_t \boldsymbol{\beta}_{ex} + \boldsymbol{\varepsilon}_t. \quad (5)$$

Here, \mathbf{X}_t^{\otimes} is the vector of all unique two-way interactions (i.e., products) between the elements of $(X_t, \bar{\mathbf{X}}_t^{\ell^X})$, and \mathbf{Y}_t^{\otimes} is the vector of all unique two-way interactions between the elements of $(X_t, \bar{\mathbf{Y}}_t^{\ell^Y})$. Equation (5) can be considered both a special case and generalization of a vector autoregressive model; the former because it involves only two three series, one of which is exogenous, and the latter because of the interaction terms.

To aid future statistical methods development, note that the ARCO model can be generalized as part of the exponential family by treating its linear component as η , the linear predictor of a generalized linear model (GLM). Specifically, let $\eta_{ARCO} = \beta_0 + \beta_X X_t + \bar{\mathbf{X}}_t^{\ell^X} \boldsymbol{\beta}_{co} + \mathbf{X}_t^{\otimes} \boldsymbol{\beta}_{Xco} + \bar{\mathbf{Y}}_t^{\ell^Y} \boldsymbol{\beta}_{ar} + \mathbf{Y}_t^{\otimes} \boldsymbol{\beta}_{Xar} + \mathbf{V}_t \boldsymbol{\beta}_{ex}$. Then the dynamic regression models of Vieira et al (2017) [25] can be considered a special case of the resulting *generalized ARCO* model, with a binary outcome and the canonical logit link function.

Throughout the rest of this paper, we will often specify our structural causal model $g(X_t, \bar{\mathbf{Y}}_t^{\ell^Y}, \bar{\mathbf{X}}_t^{\ell^X}, \mathbf{W}_t, \boldsymbol{\varepsilon}_t)$ using the ARCO model. We will also assume that $\{(\mathbf{W}_t)\}$ is WSS unless otherwise stated.

2.11 ARCO in an N-of-1 Experiment

We now derive three long-run averages implied by an ARCO model of lag order 1 (here, with $\bar{\mathbf{X}}_t^{\ell^X} = X_{t-1}$ and $\bar{\mathbf{Y}}_t^{\ell^Y} = Y_{t-1}$) when X is randomized at every period as in an n-of-1 experiment. These averages will allow us to identify and estimate the APTE directly using this simple model's parameters, which we will use in a brief simulation study in Section 4. However, to fit more flexible models for use in APTE discovery, we require a model-agnostic approach to estimate the APTE. Model-twin randomization is just such an approach, which we will introduce in a later section.

This order-1 model is $Y_t = Y_t^{X_t X_{t-1} \bar{\mathbf{X}}_{t-1}} = \beta_0 + \beta_X X_t + \beta_{co} X_{t-1} + \beta_{Xco} X_t X_{t-1} + \beta_{ar} Y_{t-1} + \beta_{Xar} X_t Y_{t-1} + \mathbf{V}_t \boldsymbol{\beta}_{ex} + \boldsymbol{\varepsilon}_t$. This is because of the implicit recursive dependence of Y_t on the exposure history beyond $t-1$; i.e., Y_{t-1} is a function of X_{t-2} and Y_{t-2} , Y_{t-2} is a function of X_{t-3} and Y_{t-3} , etc.

In general, we have $E(Y_t | X_t = x_t) = \beta_0 + \beta_X x_t + \beta_{co} E(X_{t-1} | X_t = x_t) + \beta_{Xco} x_t E(X_{t-1} | X_t = x_t) + \beta_{ar} E(Y_{t-1} | X_t = x_t) + \beta_{Xar} x_t E(Y_{t-1} | X_t = x_t) + E(\mathbf{V}_t | X_t = x_t) \boldsymbol{\beta}_{ex}$. Now suppose X is always randomized with probability $\Pr(X = 1) = \pi$ such that $E(X_{t-1} | X_t = x_t) = E(X_{t-1}) = \Pr(X_{t-1} = 1) = \pi$, $E(Y_{t-1} | X_t = x_t) = E(Y_{t-1})$, and $E(\mathbf{V}_t | X_t = x_t) = E(\mathbf{V}_t)$. Furthermore, $E(Y_{t-1}) = E(Y) = \mu_Y$ because $\{Y_t\}$ is WSS; likewise, $E(\mathbf{V}_t) = \boldsymbol{\mu}_V$.

Finally, recall from equation (4) that $E(Y_t | X_t = x_t) = Y_t^{x^*}$. Hence, long-run effect constancy holds because $\delta_t^{\text{PTE}} = Y_t^{1^*} - Y_t^{0^*} = E(Y_t | X_t = 1) - E(Y_t | X_t = 0) = \beta_X + \beta_{Xco} \pi + \beta_{Xar} \mu_Y$ is constant across all periods in the long run. We therefore have $\delta^{\text{APTE}} = \beta_X + \beta_{Xco} \pi + \beta_{Xar} \mu_Y$ by (3). After re-arranging terms, we also have $E(Y_t | X_t = x_t) = \alpha + x_t \delta^{\text{APTE}}$ where $\alpha = \beta_0 + \beta_{co} \pi + \beta_{ar} \mu_Y + \boldsymbol{\mu}_V \boldsymbol{\beta}_{ex}$.

When the APTE is not modified by carryover such that $\beta_{Xco} = 0$, and is not modified by past outcomes such that $\beta_{Xar} = 0$, it just reflects the impact of X_t through β_X . If carryover's modifying influence is positive such that $\beta_{Xco} > 0$, this amplifies the impact of X_t in proportion to the probability that $X_t = 1$; a negative influence dampens its impact. For completeness, in an n-of-1 experiment we have the long-run mean outcome

$$\mu_Y = \frac{\beta_0 + \beta_X \pi + \beta_{co} \pi + \beta_{Xco} \pi^2 + \boldsymbol{\mu}_V \boldsymbol{\beta}_{ex}}{1 - \beta_{ar} - \beta_{Xar} \pi}.$$

See the Appendix for the derivation.

2.12 ATEs and APTEs and HAPTEs, Oh My!

At this point, we should pause to appreciate the importance of the question answered by the APTE. The HAPTE is useful to a self-tracker interested primarily in past effects given their past behavior. This is fine if their goal is mainly to diagnose what already happened. However, if the self-tracker's goal is treatment or intervention by first understanding the effect or impact in order to change the outcomes by changing their behavior (i.e., not replicate the same exposure history), the HAPTE may not be the appropriate estimand.

The APTE question of “what might the effect be in an n-of-1 experiment” is less intuitive than the one posed earlier: “What is a possible sustained effect of X on Y , that I might be able to modify?” However, we must first develop the fundamental theory for this “toy example” before tailoring it to answer the useful questions like the latter.

The quantity δ^{APTE} also highlights the crucial difference in interpretation between the APTE and the ATE. This APTE is a type of *expected average treatment effect* as defined in Sävje et al (2021) [63]. To paraphrase the authors, the APTE “captures the expected effect of changing a random period’s treatment if the current study had been an n-of-1 experiment, with its particular history of unchangeable, exogenous characteristics.”

Contrast this with the ATE, which is the average effect of changing *all participants’ treatments* from $X = 1$ to $X = 0$. Applying this approach to our time series data would involve assigning $X = 1$ and $X = 0$ at all periods, and comparing the predicted mean potential outcomes under each treatment level. This ATE-type procedure would help answer a related but different question: “What would have been the average effect of changing *the treatment to the same level over all periods* if the current study had been an n-of-1 experiment, with its particular history of unchangeable, exogenous characteristics.”

This key distinction foreshadows how the model-twin randomization procedure estimates the APTE (explained in Section 3.3), compared to how the analogous ATE-type procedure above works. Briefly, model-twin randomization is a Monte Carlo method that randomly shuffles the exposure vector over all periods, predicts potential outcomes under each treatment level, adds random noise for better statistical comparison, compares the average predicted noisy outcomes under each treatment level, and then repeats this procedure multiple times until convergence. In contrast, the ATE-type procedure above simply changes all treatments to 1 or 0 in order to compare outcomes (possibly with noise added).

2.13 Other Temporal Considerations

In an n-of-1 trial, carryover might be avoided in PTE estimation by using a *washout period* that allows the lingering influence of past treatment to “wash out” of the participant’s system [5]. This is often done by design, through analytic adjustment, or both. The physical or design-based washout approach involves not administering the next treatment assignment until the influence of the previous treatment assignment has subsided. The analytic washout approach involves down-weighting or dropping time points at which carryover still exists.

In our example, an example of either approach involving dropping time points involves only including t at which $X_{t-1} = 0$ (assuming $X = 0$ denotes the baseline treatment at which the outcome is at a baseline level). This constrains the PTE to just $Y_t^{10} - Y_t^{00} = \beta_X$ regardless of whether carryover modifies the overall PTE that allows for carryover. In this paper, we will assume we cannot designate a washout period a priori, and so must instead include any treatment history with potential carryover in our models.

If the participant is measured multiple times during a period or phase such that we have $j \in \{1, \dots, m_t\}$ repeated measurements per period t , there is an opportunity to assess and adjust for *slow onset or decay* of the treatment effect. A treatment with slow onset takes time to reach its maximum or stable PTE, which may span more than one period. Similarly, a treatment with slow decay takes time to dissipate or wash out. If its washout time spans more than one period, then carryover exists. Multiple measurements per phase are standard practice in SCEDs. In studies that define a day as a period, intraday sensor measurements (as with a Fitbit or Apple Watch) are taken over uniform time intervals commonly called *epochs*.

Slow onset and decay is a topic beyond the scope of this paper, and we will assume henceforth that there is no slow onset or decay. Still, in Section 6 we will propose a sketch of a longitudinal-based approach to model such intraday trends, with which to estimate an APTE that reflects a within-period trend.

3 Estimation Methods

In an n-of-1 trial, randomization eliminates confounding due to autocorrelation and carryover. There is no such guarantee in an n-of-1 observational study; the possibility of confounding cannot be ignored. Thankfully, a number of methods exist to address or adjust for confounding in nomothetic studies, thereby to estimate the ATE.

We will implement one such approach that Daza (2018) [24] adapted for estimating the APTE. This *g-formula* approach (see below) directly adjusts for autocorrelation- and carryover-induced confounding. Readers interested in the underlying theory should review that article. In this paper, we will propose an implementation of this approach.

3.1 Two Common Approaches

Recall that to estimate the ATE, we can estimate $E(Y^x)$ directly if X is randomized by estimating $E(Y|X = x)$ using only observed values. We need not directly model the outcome mechanism $Y = g(X, \mathbf{W}, \mathcal{E})$ using an *outcome model*). This follows from the law of total expectation,

$$\begin{aligned} E(Y|X = x) &= E_{\mathbf{W}} \{E(Y|X = x, \mathbf{W}) | X = x\} \\ &= E_{\mathbf{W}} \{E(Y|X = x, \mathbf{W})\} \text{ if } X \text{ is randomized} \\ &= E(Y^x) \text{ by (1)}. \end{aligned} \tag{6}$$

Specifically, this result explains why we can simply infer $E(Y^x)$ from our estimate $\hat{E}(Y|X = x)$ when X is randomized, without having to model $E(Y|X = x, \mathbf{W})$. Nonetheless, we could still fit an outcome model to correctly estimate the ATE (i.e., using an asymptotically consistent estimator).

First, note that fitting an outcome model is the ubiquitous practice in both statistical and machine learning settings; explicitly in the former, implicitly in the latter as the prediction function $Y \sim f(X, \mathbf{W})$. From Section 2.1, note that thanks to causal consistency, the outcome mechanism is related to the PO mechanism as $Y = g(X, \mathbf{W}, \mathcal{E}) = \sum_{\{s\}} g_s(\mathbf{W}, \mathcal{E}) I(X = s)$, with shorthand $Y = g_X(\mathbf{W}, \mathcal{E})$. Hence, we can model either the outcome mechanism $g(X, \mathbf{W}, \mathcal{E})$ or PO mechanism $g_X(\mathbf{W}, \mathcal{E})$ because both are mathematically identical (specifically, for a given value of X).

In our procedure, we would fit the correct outcome model to our observed values, and thereby estimate the conditional mean $E(Y|X = s, \mathbf{W}) = E_{\mathcal{E}}(g(X, \mathbf{W}, \mathcal{E})|X = s, \mathbf{W})$ for each exposure level s . To illustrate, recall our early example in Section 2.1 with $g(X, \mathbf{W}, \mathcal{E}) = \beta_0 + \beta_1 X + \mathbf{W}\beta_2 + \mathcal{E}$. We would first estimate the parameters $\{\beta_0, \beta_1, \beta_2\}$ with which to estimate $E(Y|X = s, \mathbf{W})$. For each $s \in \{0, 1\}$, we would then predict outcome values as \hat{Y}_i^s for all study participants $i = 1, \dots, n$. Following equation (6), we would then estimate $E(Y^s)$ by averaging over all predicted values for each $s \in \{0, 1\}$; i.e., $\bar{\hat{Y}}^s = \frac{1}{n} \sum_{i=1}^n \hat{Y}_i^s$. Finally, we would estimate the ATE as the difference between these averages; i.e., $\bar{\hat{Y}}^1 - \bar{\hat{Y}}^0$.

But this procedure also works for estimating $E(Y^x)$ *even if X is not randomized!* This surprising result is the key insight underlying the well-established method known as the *g-formula* or *g-computation formula*, also known as direct standardization, stratification, regression adjustment, and the back-door adjustment formula [64, 65, 66, 67, 68, 69, 70]. The g-formula is simply the equivalence of the last two lines of equation (6). Intuitively, it states that if we have observed all confounders and know the outcome mechanism, then we can correctly estimate the ATE by replicating the probability conditions for the corresponding hypothetical RCT.

What if we do not know enough about how to model the outcome? If instead we can specify a reasonably correct *propensity model* for $\Pr(X = s|\mathbf{W})$, the propensity of seeing $X = s$ for a given level of W , then we can use a number of *propensity score* methods [47, 66, 71] to estimate the ATE. These include the matching and IPW approaches mentioned in Section 2.3. In this approach, $X = I(\mathcal{E}^X > \Pr(X = 1|\mathbf{W}))$ where \mathcal{E}^X is uniformly distributed between 0 and 1. This technique is inspired by Horvitz-Thompson weights used in survey sampling [72, 73].

Our main focus will be to characterize the performance (with respect to empirical bias) of a g-formula estimation approach. However, we will also propose a complementary IPW method for comparison. We will not explore *doubly robust* methods (e.g., “augmented IPW”), which involve specifying both outcome and propensity models. They are called as such because only one of these two models needs to be specified correctly to guarantee consistent estimation [74].

3.2 Modeling Flexibility

Now suppose the outcome and propensity mechanisms are either unknown or cannot otherwise be reasonably justified (e.g., due to a lack accumulated theoretical evidence). This is the case in our setting of causal hypothesis generation: Our primary objective is to *identify, select, or propose* plausible models for a small set of posited causal effects, rather than *estimate* effects and associations posited by scientifically defensible or otherwise well-established a priori models [75, 76].

Note that the outcome mechanism in equation (6) can take any appropriate functional form. These have traditionally been modeled using linearized parametric or semi-parametric models in the statistics literature. However, (6) applies to the true mechanism, which may or may not be a linearized model. Hence, we can also use supervised learning methods that allow us to fit models focused on characterizing the relationship between X , the exposure of interest, and the outcome Y , while also flexibly accommodating non-exposure variables \mathbf{W} . Likewise holds for modeling the propensity of X .

The decision tree method is one such non-parametric approach, that Athey and Imbens (2015) [77] used to estimate a conditional ATE for a continuous outcome (specified as a difference between mean POs). Their tree-based approach can be used to estimate an APTE if conditional WSS holds (i.e., the outcomes are WSS conditional on the causes). WSS replaces the assumption of conditional independence (i.e., the outcomes are mutually independent conditional on the causes) needed for consistent effect estimation. Unlike linearized models that require prespecification of interaction terms, the tree-based method known as random forests (RF) is able to implicitly allow for multiple interactions between predictors in predicting the outcome; hence, its appeal.

Following Athey and Imbens (2015) [77], we will take a Single Tree approach, and model the outcome as a function of both the exposure and other causes using RF. For comparison, their Two Trees approach for conducting feature selection (i.e., for non-exposure causes important for predicting potential outcomes) involves fitting separate outcome models for each exposure level. To model the exposure propensity, we will simply model the propensity directly (versus their more sophisticated Transformed Outcome Tree approach).

3.3 Model-Twin Randomization

Section 2.12 motivated the need to take a sequential approach to implementing the g-formula for estimating the APTE. To review, the outcome Y_t is sequentially generated, unlike the outcome Y_i generated across participants in ATE-focused settings.

In this section, we propose a sequential approach for numerical estimation called model-twin randomization (MoTR). MoTR randomizes the originally observed sequential exposure $\{(x_t)\}$, thereby changing it from a possibly endogenous variable (i.e., that might be affected by past values of Y) into an exogenous one unaffected by the outcome. Hence, MoTR is a Monte Carlo method that provides numerically approximate calculations of statistically consistent estimates of the APTE, along approximate confidence intervals (CIs) for conducting inference.

Here is the general procedure.

1. Fit the outcome model $\mu_t = E(Y_t|X_t, \mathbf{W}_t)$ to the observed data $\{(x_t), (\mathbf{w}_t)\}$. The estimator $\hat{\mu}_t$ from fitting the model is the participant’s *model twin*—a digital twin that represents the participant’s outcome mechanism for estimating the APTE.
2. Run the model twin through a simulated n-of-1 trial by “running the MoTR” as follows. For run (i.e., iteration) r :
 - (a) Randomly permute or shuffle all observed x_t . Let $\mathbf{X}_r = (X_{r1}, \dots, X_{rm})$ represent this randomized sequence. This step preserves the original ratio of exposures to non-exposures, reflecting the exposure’s observed overall propensity.
 - (b) Generate \mathbf{W}_{rt} at each period t sequentially as follows. We need to index this matrix by its run number r because some of its components will change with each run, as detailed below.
 - i. Keep any exogenous variables \mathbf{v}_t contained in \mathbf{w}_t equal to their corresponding values in \mathbf{W}_{rt} .
 - ii. Set all lags of Y_t contained in \mathbf{W}_t equal to their values generated in past runs. For example, set Y_{t-1} equal to $\hat{Y}_{r(t-1)}$ as defined in step (c).

- iii. Set all lags of X_t contained in \mathbf{W}_t equal to their corresponding values in \mathbf{X}_r .
 - (c) Generate Y_{rt} at each period t sequentially as follows.
 - i. Predict the outcome as $\hat{\mu}_{rt} = \hat{E}(Y_t | X_t = X_{rt}, \mathbf{W}_t = \mathbf{W}_{rt})$.
 - ii. Add random noise to each predicted value as $\hat{Y}_{rt} = \hat{\mu}_{rt} + \varepsilon_{rt}$. Here, $\varepsilon_{rt} \sim N(0, \sigma_\varepsilon)$ where σ_ε is the standard deviation of the residuals ($\{Y_t - \hat{\mu}_t\}$) (treated as fixed); $\hat{\mu}_t$ is the predicted mean outcome conditional on the observed data $\{x_t, \mathbf{w}_t\}$. This step preserves summary information about residual variation in the outcome, as is commonly done to create prediction intervals in statistics.
 - iii. Note that \hat{Y}_{rt} may be an element of $\mathbf{W}_{rt'}$ for some future period $t' > t$.
 - (d) For $s \in \{0, 1\}$, estimate $E(Y^s)$, the mean PO, as the average of the noisy predicted outcomes; i.e., $\tilde{Y}_r^s = \frac{1}{m_s} \sum_{t=1}^m \hat{Y}_{rt} I(X_{rt} = s)$ where $m_s = \sum_{t=1}^m I(X_t = s)$, which is constant regardless of r . Estimate the APTE as $\hat{\delta}_r^{\text{MoTR}} = \tilde{Y}_r^1 - \tilde{Y}_r^0$.
 - (e) Estimate the corresponding CI likewise; e.g., do this using the common t-test if the predicted outcomes are fairly normally distributed.
 - (f) Calculate the cumulative average APTE over all previous runs as the average of all estimates $\hat{\delta}_r^{\text{MoTR}}$ up to and including the current run r ; i.e., $\hat{\delta}_r^{\text{MoTR}} = \frac{1}{r} \sum_{h=1}^r \hat{\delta}_h^{\text{MoTR}}$. Calculate the cumulative average CI likewise.
3. Repeat steps 2(a)-2(e) until all three cumulative averages converge based on reasonable criteria. To ensure some stability in cumulative estimates, consider setting a minimum r_{\min} such that $r_{\min} \leq r$. To save on computation time, consider setting a maximum r_{\max} such that $r \leq r_{\max}$.
 4. Report the final values from step 3 as the APTE estimate $\hat{\delta}^{\text{MoTR}}$ along with its CI.

3.4 Propensity Score Twin

In this section, we propose an IPW approach to complement MoTR, called propensity score twin (PSTn, pronounced ‘‘piston’’). Unlike MoTR, PSTn is not a sequential Monte Carlo method. Instead, PSTn only predicts the exposure probability at each period once after modeling the probability of exposure; i.e., $\Pr(X_t = s | \mathbf{W}_t)$. As this is not the focus of our paper, we will limit our characterization to bias in PSTn estimation; we will not characterize inference, which requires estimating CIs.

Here is the general procedure.

1. Fit the propensity model $\pi_t = \Pr(X_t = 1 | \mathbf{W}_t)$ to the data. Similar to MoTR, the estimator $\hat{\pi}_t$ from fitting the model is the participant’s *propensity score twin*—a digital twin that represents the participant’s exposure mechanism for estimating the APTE.
2. Weight each observed Y_t by the reciprocal of its corresponding estimated propensity based on the observed exposure; i.e., $\tilde{Y}_t = Y_t / \{x_t \hat{\pi}_t + (1 - x_t)(1 - \hat{\pi}_t)\}$. Consider applying the following adjustments to mitigate overly large weights resulting from overly small estimated propensities.
 - (a) Only use trimmed $\hat{\pi}_t$ values (i.e., drop extreme $\hat{\pi}_t$ values).
 - (b) Only use overlapping $\hat{\pi}_t$ values (i.e., keep the range of $\hat{\pi}_t$ values with the most overlap between groups with $s \in \{0, 1\}$).
 - (c) Use stabilized weights (i.e., multiply \tilde{Y}_t by the proportion of the sample with $X = x_t$ for the corresponding value of x_t) [78].
3. For $s \in \{0, 1\}$, estimate $E(Y^s)$ as the average of the weighted outcomes; i.e., $\tilde{Y}^s = \frac{1}{m_s} \sum_{t=1}^m \tilde{Y}_t I(X_t = s)$.
4. Estimate the APTE as $\hat{\delta}^{\text{PSTn}} = \tilde{Y}^1 - \tilde{Y}^0$.

4 Simulation Study

In this section, we describe how we used simulated data to characterize the empirical bias of the MoTR and PSTn estimators ($\hat{\delta}^{\text{MoTR}}$ and $\hat{\delta}^{\text{PSTn}}$, respectively). We characterized this bias when each model was correctly specified as the true data-generating mechanism, which we specified as a GLM (i.e., ARCO for the outcome, logistic for the exposure). We also characterized this bias using naive APTE estimation methods; i.e., when no modeling was done, and when the true models were fit but were not adjusted for confounding by either method.

Finally, we characterized the empirical bias of the RF approaches of section 3.2. We expected that RF, while more flexible than linearized models in useful ways (see Section 3.2), would be more biased because the relevant prediction function is not identical to the true GLM mechanism.

4.1 Data-generating Procedure

EJD collected 222 days of sleep duration and step-count data using a Fitbit Charge 3 wrist-worn sensor. Hence, each synthetic (i.e., simulated) dataset we generated had $m = 222$ time points.

We specified our outcome and exposure of interest as follows. A period was specified as a day. Our outcome was daily total sleep time (TST), defined as the total number of hours asleep per night. Our physical-activity exposure was the daily number of steps per minute awake. We chose this rather than daily raw step count because we wanted to understand if increasing physical activity overall—regardless of how much time the participant was awake—led to longer or shorter sleep. However, simply getting more sleep leaves one less time to take steps the following day. Hence, raw step count is often associated with sleep duration [46], regardless of how it might affect sleep duration (i.e., our APTE of interest).

In the standard potential outcomes framework, it is reasonable to dichotomize continuous exposures in order to define clear causal effects between distinct groups or levels. Hence, we dichotomized our exposure into high and low physical activity based on the observed median steps per minute over all 222 days of observation.

We generated each synthetic dataset (indexed h) using the following procedure, which induces autoregression and confounding via endogeneity (as might be present in real data).

1. If $t = 1$, generate Y_{ht} as a continuous variable drawn from $\beta_0 + \mathcal{E}_t$ where $\mathcal{E}_t \sim N(0, \sigma_\varepsilon)$. Otherwise, proceed to the next step.
2. For both $s = 0$ and $s = 1$, generate Y_{ht}^s using the ARCO PO mechanism $Y_{ht}^s = \beta_0 + \beta_X s + \beta_{ar} Y_{t-1} + \mathcal{E}_t$ where Y_{t-1} is set equal to $Y_{h(t-1)}$.
3. If $t = 1$, generate $X_{ht} \in \{0, 1\}$ as a binomial variable with probability $\pi_1 = \Pr(X_1 = 1)$. Otherwise, generate X_{ht} using the propensity mechanism $\text{logit}(\pi_t) = \alpha_0 + \alpha_{en} Y_{t-1}$ where $\pi_t = \Pr(X_t = 1 | Y_{t-1})$, and where Y_{t-1} is set equal to $Y_{h(t-1)}$. Here, $\alpha_{en} \neq 0$ induces endogeneity by making X_t depend on Y_{t-1} .
4. Generate the observed outcome Y_{ht} using causal consistency. That is, generate $Y_{ht} = Y_t^1 X_t + Y_t^0 (1 - X_t)$ where Y_t^s is set equal to Y_{ht}^s for both $s = 0$ and $s = 1$, and where X_t is set equal to X_{ht} .

The parameters we used were $\beta_0 = 2$, $\sigma_\varepsilon = 0.5$, $\beta_X = 1.1$, $\beta_{ar} = 0.8$, $\pi_1 = 0.5$, $\alpha_0 = -0.25$, and $\alpha_{en} = 1.25$. Note that Y_{ht}^s is stationary because $|\beta_{ar}| \leq 1$; hence, the true APTE was $\beta_X = 1.1$.

4.2 Analysis Methods and Results

The six estimation methods we used are listed in Table 3. We used $r = 200$ MoTR runs, and applied trimming and overlapping to our propensity scores (which we stabilized). The coefficient estimate method was included as an extra coding check that our code was correct; i.e., we expected it to be unbiased over many simulations.

The coefficient estimate, MoTR-GLM, and PSTn-GLM methods all involved fitting the correct models (i.e., the correct ARCO-outcome or exposure mechanisms in Section 4.1). Specifically, for both the coefficient

Table 3: Simulation study analysis methods.

Method	Estimator	Description	Bias Expected
Raw comparison of averages (i.e., no modeling)	$\hat{\delta}^{\text{raw}}$	$\frac{1}{m_1} \sum_{t=1}^m Y_t I(X_t = 1) - \frac{1}{m_0} \sum_{t=1}^m Y_t I(X_t = 0)$	yes
Coefficient estimate	$\hat{\beta}_X$	GLM estimator of ARCO exposure coefficient	no
MoTR-GLM	$\hat{\delta}^{\text{MoTR-GLM}}$	$\hat{\delta}^{\text{MoTR}}$ after fitting GLM outcome model	no
PSTn-GLM	$\hat{\delta}^{\text{PSTn-GLM}}$	$\hat{\delta}^{\text{PSTn}}$ after fitting GLM propensity model	no
MoTR-RF	$\hat{\delta}^{\text{MoTR-RF}}$	$\hat{\delta}^{\text{MoTR}}$ after fitting RF prediction function	some
PSTn-RF	$\hat{\delta}^{\text{PSTn-RF}}$	$\hat{\delta}^{\text{PSTn}}$ after fitting RF prediction function	some

Table 4: Simulation study analysis results for one synthetic dataset with a true APTE of 1.1.

Method	Estimate (95% CI)
Raw comparison	0.35 (0.1, 0.6)
Coefficient estimate	1.10 (0.92, 1.27)
MoTR-GLM	1.08 (0.68, 1.48)
PSTn-GLM	0.98
MoTR-RF	0.69 (0.4, 0.98)
PSTn-RF	0.94

and MoTR-GLM methods, we fit the outcome model $Y_t = \beta_0 + \beta_X X_t + \beta_{ar} Y_{t-1} + \mathcal{E}_t$ where $\mathcal{E}_t \sim N(0, \sigma_\epsilon)$. For the PSTn-GLM method, we fit the propensity model $\text{logit}(\pi_t) = \alpha_0 + \alpha_{en} Y_{t-1}$ where $\pi_t = \Pr(X_t = 1 | Y_{t-1})$.

The RF methods involved fitting prediction functions. For the MoTR-RF method, we fit the prediction function $Y_t \sim f(X_t, Y_{t-1})$. For the PSTn-RF method, we fit the classification function $X_t \sim f(Y_{t-1})$.

To start understanding how the raw, MoTR, and PSTn methods relate to each other, the results of analyzing one synthetic dataset (i.e., $h = 1$) are shown in Figure 1. Here, the correct models were used for MoTR and PSTn, with a sample size of $m = 220$. The corresponding values of each final estimate at run $r = 200$ are shown in Table 4.

For this particular dataset, the MoTR and PSTn methods estimate the true APTE with little bias compared to the raw comparison when their models are specified correctly. The MoTR CI even covers the true APTE. However, the MoTR method that uses RF is more biased than the corresponding PSTn method. This seemingly puzzling result was the result of random sample-to-sample variation, as seen in the empirical bias results over 100 synthetic datasets shown in Figure 2. This approach is a way of approximating the true bias of an estimator at a given sample size.

Over 100 datasets, we see in Figure 2 that the empirical bias for the raw comparison method is the largest compared to the coefficient estimate, MoTR-GLM, and PSTn-GLM methods, while PSTn-GLM performs worse than MoTR-GLM. The coefficient estimate method is unbiased, as expected, confirming that our modeling code was correct. For the RF-based methods, both MoTR-RF and PSTn-RF perform better than raw comparison. However, MoTR-RF performs worse than MoTR-GLM, as expected. Likewise holds for PSTn-RF, which also is less consistent in that its results vary widely more from sample to sample, as evidenced by its wider spread of points and CI.

We also increased the sample size to $m = 730$. This allowed us to begin to assess the asymptotic trend in bias of each estimator implied by the central limit theorem (CLT). Appendix Figure A1 shows that the all estimators except PSTn-GLM exhibit similar bias as they do in the smaller sample. PSTn-GLM in fact performs better (i.e., with reduced empirical bias), as expected under the CLT.

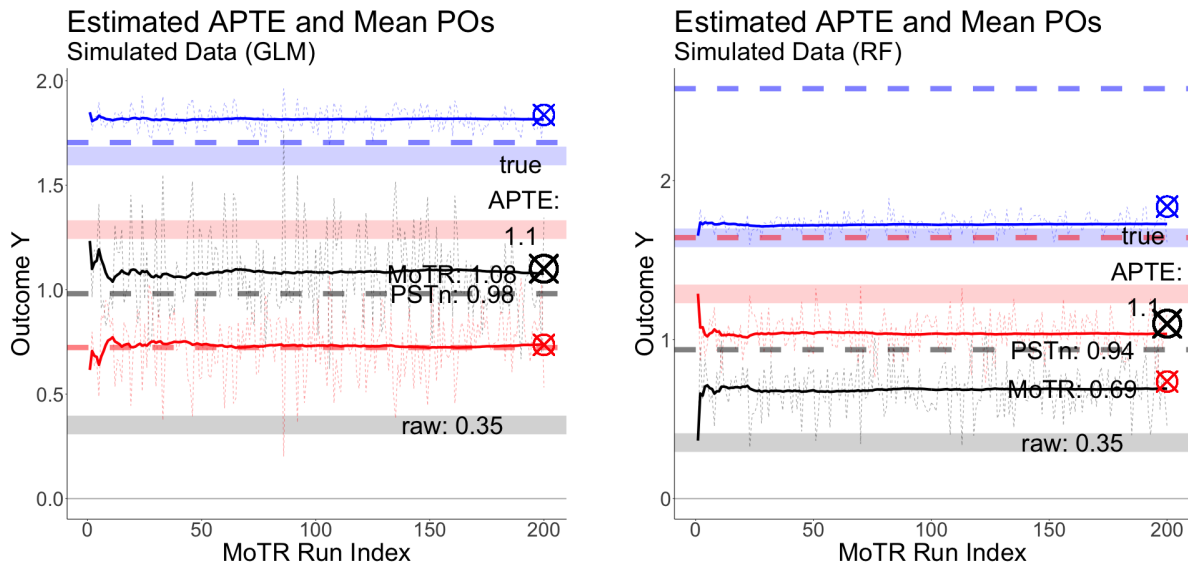


Figure 1: Analysis results of applying each method to one synthetic dataset; i.e., generalized linear model (GLM) or random forests (RF). MoTR used $r_{min} = 10$ to $r_{max} = 200$ runs. *Legend:* The thin dashed black line represents each MoTR run's APTE estimate. The solid black line represents the MoTR estimate (i.e., cumulative over all previous APTE estimates). The thicker dashed black (grey) line represents the PSTn estimate. The thick, faded black (grey) line represents the raw comparison estimate. The blue and red sets of lines represent the estimated mean potential outcomes (POs) under high and low exposure levels, respectively, for each of the three estimators. (The difference between the blue and red lines equals the corresponding black line for any run.) The circled X's mark the true mean PO and APTE values.

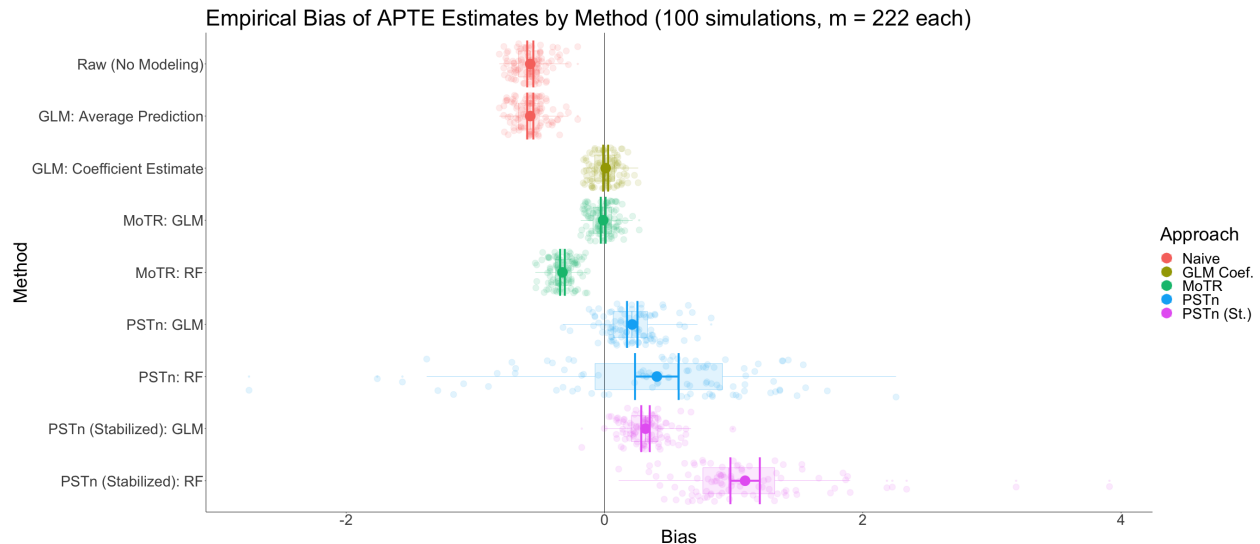


Figure 2: Analysis results of applying each method to 100 synthetic datasets with $m = 220$. Each light dot represents the empirical bias of one synthetic dataset for estimating a true APTE of 1.1. Each dark dot represents the average empirical bias over all 100 datasets, with corresponding 95% confidence interval shown as symmetric error bars.

Table 5: Empirical study analysis results.

Method	Estimate (95% CI)	Estimated Steps per Minute (95% CI)
Raw comparison	0.09 (0.02, 0.16)	1.23 (1.05, 1.45)
MoTR-GLM	0 (-0.07, 0.07)	1 (0.851, 1.17)
PSTn-GLM	0.15	1.41
MoTR-RF	0.03 (-0.05, 0.1)	1.07 (0.891, 1.26)
PSTn-RF	0.22	1.66

5 Empirical Study

In this section, we describe how we estimated an APTE of EJD’s nightly TST on his steps per minute the next day. In our models, we included an indicator for weekend (versus weekday), which we treated as an exogenous variable. To reflect the fact that we would not be able to modify the day of the week in a hypothetical n-of-1 trial, we did not modify its original values. Hence, our estimand was that of (3)—a conditional APTE.

As with the simulation study of Section 4, we analyzed $m = 222$ days of EJD’s sleep duration and step-count data using a Fitbit Charge 3 wrist-worn sensor, collected from May 2019 through December 2020. We transformed the raw outcome, steps per minute the next day, by taking its log (base 10); this was the outcome we analyzed. We did this to ensure the outcomes were fairly normally distributed, to meet the GLM modeling assumption of normally distributed residuals. We dichotomized our exposure, nightly TST, based on the observed median over all 222 days of observation of 7.1 hours; i.e., high TST corresponded to > 7.1 hours of sleep on a given night, and otherwise the exposure was labeled as low TST.

We used the same six estimation methods listed in Table 3, except for the coefficient estimate method (which we’d previously used just to check that our modeling code was correct). As with our simulation study, we used $r = 200$ MoTR runs, and applied trimming and overlapping to our stabilized propensity scores. For all four methods, \mathbf{W}_t consisted of the endogenous variables X_{t-1} and Y_{t-1} (or \mathbf{Q}_{t-1} , explained below), and the exogenous variable V_t where $V_t = 1$ if day t is a weekend (and $V_t = 0$ otherwise).

We fit the following MoTR models. For the MoTR-GLM method, we fit the outcome model $Y_t = \beta_0 + \beta_X X_t + \beta_{co} X_{t-1} + \mathbf{Q}_{t-1} \boldsymbol{\beta}_{ar} + \beta_{ex} V_t + \mathcal{E}_t$ where $\mathcal{E}_t \sim N(0, \sigma_\varepsilon)$. Here, \mathbf{Q}_{t-1} is a 1×4 vector of zeroes and ones indicating the quartile of $(\{Y_i\})$ that Y_{t-1} fell into (along with conformable coefficient 4×1 vector $\boldsymbol{\beta}_{ar}$). For example, $\mathbf{Q}_{t-1} = (0, 0, 1, 0)$ if Y_{t-1} is in the third quartile. We did this to allow for a more flexible non-linear relationship between the current and lagged outcome, at the expense of losing continuous-valued predictor information. For the MoTR-RF method, we fit the prediction function $Y_t \sim f(X_t, X_{t-1}, Y_{t-1}, V_t)$. Note that we used Y_{t-1} instead of \mathbf{Q}_{t-1} because RF automatically segments or partitions these continuous values, precluding our need to do so manually. MoTR used $r_{min} = 10$ to $r_{max} = 200$ runs. MoTR performance over all runs is shown in Appendix Figure A2, which parallels Figure 1.

We fit the following PSTn models. For the PSTn-GLM method, we fit the propensity model $\text{logit}(\pi_t) = \alpha_0 + \alpha_{ar} X_{t-1} + \alpha_{en} \mathbf{Q}_{t-1} + \alpha_{ex} V_t$ where $\pi_t = \Pr(X_t = 1 | X_{t-1}, \mathbf{Q}_{t-1}, V_t)$. For the PSTn-RF method, we fit the classification function $X_t \sim f(X_{t-1}, Y_{t-1}, V_t)$.

The results are shown in Table 5. We estimated that under high TST, EJD took 1.23 more steps per minute than he did under low TST. However, if our outcome model was identical to the true outcome mechanism, then getting more sleep (i.e., high TST) increased EJD’s physical activity (versus low TST) by an average of only 1 step per minute. That is, 1.23 would have been a naive overestimate of the APTE of sleep duration on physical activity. Using the more flexible RF method yielded qualitatively similar results.

If instead our propensity model was identical to the true propensity mechanism, then getting more sleep increased EJD’s physical activity by an average of 1.41 steps per minute. In this case, 1.23 would have been a naive underestimate of the APTE of sleep duration on physical activity. As with MoTR, the RF method yielded qualitatively similar results.

6 Discussion

We presented a new method, model-twin randomization, to estimate the average period treatment effect using wearable sensor data. We then estimated the daily APTE of sleep duration on steps per minute using 222 days of EJD’s Fitbit data.

The contradiction in APTE estimates between MoTR and the propensity-score based method “propensity score twin” results highlights the importance of specifying the model as close to the true mechanism as possible. This should be done both empirically (i.e., in a data-driven way; for example, through parameter tuning and model selection) and scientifically (i.e., based on related literature). They provide a real example of why researchers sought to develop the doubly robust methods mentioned in Section 3.1.

One advanced doubly robust approach is being developed by Malenica et al (2021)[79]. They use targeted maximum likelihood estimation (TMLE) to estimate and infer the APTE. This important paper lays the theoretical groundwork for both the asymptotic consistency and normality of their TMLE estimator, and proposes a sequentially adaptive design for learning the optimal idiographic treatment rule over time. The TMLE approach also optimizes the use of machine learning models by minimizing the bias incurred when fitting such models.

MoTR provides a way to surface plausible or suggested causal effects for possible further investigation or confirmation through an n-of-1 trial. It can be used to develop a personalized idiographic intervention plan. For example, one might use the following data-driven procedure to identify combinations of models and plausible confounders that produce APTE estimates that meaningfully differ from naive estimates calculated by comparing raw averages (as in Table 3).

1. The study participant, their health provider, and the analyst decide on plausible confounders.
2. The analyst fits and selects or cross-validated initial outcome or propensity models. The analyst then selects the final models; e.g., test all selected models on a holdout set once.
3. The analyst runs MoTR or PSTn using these final models.
4. The analyst reports the findings with the largest, most statistically discernible differences (i.e., with the most statistically significant p-values) from the naive estimates. These findings may indicate situations in which confounding is strong enough to change effect estimates—and thereby change how future within-individual interventions are designed.
5. The analyst discusses the plausibility of the selected models with the study participant and their health provider to determine an intervention plan.

We are happy to report that work is already underway to deepen idiographic causal approaches in both theoretical and applied directions. These include the pioneering work of Malenica et al (2021) [79] mentioned earlier. For a recent survey of causal inference methods for time series data, see Moraffah et al (2021) [80].

Intraday sensor data can also be used to characterize average daily trends across period, analogous to longitudinal trends across individuals. In a nod to the spaghetti plots of longitudinal trend analysis, Daza (2019) [81] introduced the term *pancit plot* to describe a plot of intra-period trends. (“Pancit” is pronounced like “pun-SEAT”; it is Tagalog/Filipino for “noodles”.) Daza et al (2020) [82] illustrated pancit plots for continuous blood glucose intraday data, in which the APTE was not a scalar difference, but a difference in a daily functional trends; i.e., the difference in slope and time polynomial coefficients of a mixed-effects model to describe both the within-period trend and variability of repeated measures under each treatment condition. The clear implication is to extend APTE-based techniques (including MoTR and PSTn) to functional data analysis [83] of intensive longitudinal data.

The APTE framework was created to enable and facilitate this extension. Each time point $t(j)$ can contain sub-points (e.g., $t(j_k)$). This modularity allows for flexible temporal scaling of posited causal relationships. The framework’s utility can also be complemented and improved with formal causal diagrams such as directed acyclic graphs (DAGs) [84, 85] for conceptualizing formal structures. We are currently developing the theory needed to connect DAGs to the APTE framework.

Finally, to compare oneself to others, one might ask, how does my APTE relate to a corresponding group-level (nomothetic) ATE? One common approach is to combine APTE estimates in the same way

ATEs from multiple nomothetic studies would be aggregated in a meta-analysis (i.e., a *series-of-n-of-1*). Another approach is to use a mixed-effects model to combine and compare participant-level APTEs to the overall ATE; see the Appendix section on hierarchical models. Zucker et al (1997, 2010)[86, 87] examine these and other approaches in detail. Their work helps build a foundation with which to extend our single-subject approach for functional data analysis.

Within-individual approaches are steadily increasing in popularity due to the availability of small data and idiographic measurements. It is exciting to be able to contribute to the rigorous causal analysis of such personally meaningful data.

7 Acknowledgements

This paper was supported by EJD’s employer Evidation and LS’s employer Alphabet. Early formative work on this paper was supported by the Stanford Clinical and Translational Science Award (CTSA) to Spectrum (UL1 TR001085). The CTSA program is led by the National Center for Advancing Translational Sciences (NCATS) at the National Institutes of Health (NIH). This research was also supported by NIH grant 2T32HL007034-41 that funded EJD’s postdoctoral training. The content is solely the responsibility of the authors and does not necessarily represent the official views of the NIH.

EJD thanks the following people. Igor Matias for his constant feedback in ideation, which inspired EJD to come up with the acronym “MoTR”. Professor Linda Valeri for her helpful input on theoretical considerations. Professor Jared Huling for his direction in understanding the initially unexpected random forests results. Professor Michael Baiocchi for his constant support, feedback, and guidance. Family and friends for their constant support. Colleagues, teachers, students, and most of all, luck and privilege.

EJD dedicates this paper to Filipinos and Filipino-Americans. To all who are underrepresented or unacknowledged in science, technology, engineering, and math (STEM), and in academia: *Kaya natin ’to!* To you, the reader: Know yourself, help others, and find meaning in all things.

References

1. Estrin D. Small data, where n= me. *Communications of the ACM*. 2014;57(4):32–34.
2. Hekler EB, Klasnja P, Chevance G, Golaszewski NM, Lewis D, Sim I. Why we need a small data paradigm. *BMC medicine*. 2019;17(1):1–9.
3. Walls TA, Schafer JL. *Models for intensive longitudinal data*. Oxford University Press; 2006.
4. Matthews J. Multi-period crossover trials. *Statistical methods in medical research*. 1994;3(4):383–405.
5. Kravitz R, Duan N, the DEcIDE Methods Center N-of 1 Guidance Panel (Duan N, Eslick I, Gabler N, Kaplan H, et al. *Design and Implementation of N-of-1 Trials: A User’s Guide*. AHRQ Publication No. 13(14)-EHC122-EF. Rockville, MD: Agency for Healthcare Research and Quality; 2014. <http://www.effectivehealthcare.ahrq.gov/N-1-Trials.cfm>.
6. Senn S. Mastering variation: variance components and personalised medicine. *Statistics in medicine*. 2016;35(7):966–977.
7. Guyatt G, Sackett D, Taylor DW, Ghong J, Roberts R, Pugsley S. Determining optimal therapy—randomized trials in individual patients. *New England Journal of Medicine*. 1986;314(14):889–892.
8. Guyatt GH, Keller JL, Jaeschke R, Rosenbloom D, Adachi JD, Newhouse MT. The n-of-1 randomized controlled trial: Clinical usefulness: Our three-year experience. *Annals of Internal Medicine*. 1990;112(4):293–299.
9. Backman CL, Harris SR. Case studies, single-subject research, and n of 1 randomized trials: Comparisons and contrasts. *American Journal of Physical Medicine & Rehabilitation*. 1999;78(2):170–176.

10. Gabler NB, Duan N, Vohra S, Kravitz RL. N-of-1 trials in the medical literature: A systematic review. *Medical Care*. 2011;49(8):761–768.
11. Lillie EO, Patay B, Diamant J, Issell B, Topol EJ, Schork NJ. The n-of-1 clinical trial: The ultimate strategy for individualizing medicine? *Personalized Medicine*. 2011;8(2):161–173.
12. Duan N, Kravitz RL, Schmid CH. Single-patient (n-of-1) trials: A pragmatic clinical decision methodology for patient-centered comparative effectiveness research. *Journal of Clinical Epidemiology*. 2013;66(8):S21–S28.
13. Naughton F, Johnston D. A starter kit for undertaking n-of-1 trials. *European Health Psychologist*. 2014;16(5):196–205.
14. Nikles J, Mitchell G. *The Essential Guide to N-of-1 Trials in Health*. Springer; 2015.
15. Shamseer L, Sampson M, Bukutu C, Schmid CH, Nikles J, Tate R, et al. CONSORT extension for reporting N-of-1 trials (CENT) 2015: Explanation and elaboration. *Journal of Clinical Epidemiology*. 2016;76:18–46.
16. Vohra S, Shamseer L, Sampson M, Bukutu C, Schmid CH, Tate R, et al. CONSORT extension for reporting N-of-1 trials (CENT) 2015 Statement. *Journal of Clinical Epidemiology*. 2016;76:9–17.
17. Chen C, Haddad D, Selsky J, Hoffman JE, Kravitz RL, Estrin DE, et al. Making sense of mobile health data: an open architecture to improve individual-and population-level health. *Journal of Medical Internet Research*. 2012;14(4):e112.
18. Schork NJ. Personalized medicine: Time for one-person trials. *Nature*. 2015;520(7549):609–611.
19. Ponterotto JG. Qualitative research in counseling psychology: A primer on research paradigms and philosophy of science. *Journal of Counseling Psychology*. 2005;52(2):126–136.
20. Araujo A, Julious S, Senn S. Understanding variation in sets of N-of-1 trials. *PloS one*. 2016;11(12):e0167167.
21. Neyman J. On the application of probability theory to agricultural experiments. Essay on principles. Section 9. *Statistical Science*. 1923, tr 1990;5(4):465–480. *Translated and edited by D.M. Dabrowska and T.P. Speed from the Polish original, which appeared in Roczniki Nauk Rolniczych Tom X (1923) 1–51 (Annals of Agricultural Sciences)*.
22. Rubin DB. Estimating causal effects of treatments in randomized and nonrandomized studies. *Journal of Educational Psychology*. 1974;66(5):688–701.
23. Holland PW. Statistics and causal inference. *Journal of the American Statistical Association*. 1986;81(396):945–960.
24. Daza EJ. Causal analysis of self-tracked time series data using a counterfactual framework for n-of-1 trials. *Methods of Information in Medicine*. 2018;57(01):e10–e21.
25. Vieira R, McDonald S, Araújo-Soares V, Sniehotta FF, Henderson R. Dynamic modelling of n-of-1 data: powerful and flexible data analytics applied to individualised studies. *Health Psychology Review*. 2017;11(3):222–234.
26. Schmid CH. Marginal and dynamic regression models for longitudinal data. *Statistics in Medicine*. 2001;20(21):3295–3311.
27. Balandat M. *New tools for econometric analysis of high-frequency time series data-application to demand-side management in electricity markets*. University of California, Berkeley; 2016.
28. Hansen BB. The prognostic analogue of the propensity score. *Biometrika*. 2008;95(2):481–488.

29. Cheung Y, Qian M, Yoon S, Meli L, Diaz K, Schwartz J, et al. Are Nomothetic or Ideographic Approaches Superior in Predicting Daily Exercise Behaviors? *Methods of Information in Medicine*. 2017;56(6):452–460.
30. Burg MM, Schwartz JE, Kronish IM, Diaz KM, Alcantara C, Duer-Hefele J, et al. Does Stress Result in You Exercising Less? Or Does Exercising Result in You Being Less Stressed? Or Is It Both? Testing the Bi-directional Stress-Exercise Association at the Group and Person (N of 1) Level. *Annals of Behavioral Medicine*. 2017:1–11.
31. Wang Y. Causal Inference under Temporal and Spatial Interference. arXiv preprint arXiv:210615074. 2021.
32. Borbély AA. A two process model of sleep regulation. *Hum neurobiol*. 1982;1(3):195–204.
33. Garfield V. Sleep duration: A review of genome-wide association studies (GWAS) in adults from 2007 to 2020. *Sleep Medicine Reviews*. 2021;56:101413.
34. Kalmbach DA, Schneider LD, Cheung J, Bertrand SJ, Kariharan T, Pack AI, et al. Genetic basis of chronotype in humans: insights from three landmark GWAS. *Sleep*. 2017;40(2).
35. He Y, Jones CR, Fujiki N, Xu Y, Guo B, Holder Jr JL, et al. The transcriptional repressor DEC2 regulates sleep length in mammals. *Science*. 2009;325(5942):866–870.
36. Shi G, Xing L, Wu D, Bhattacharyya BJ, Jones CR, McMahon T, et al. A rare mutation of β 1-adrenergic receptor affects sleep/wake behaviors. *Neuron*. 2019;103(6):1044–1055.
37. Dong Q, Gentry NW, McMahon T, Yamazaki M, Benitez-Rivera L, Wang T, et al. Familial natural short sleep mutations reduce Alzheimer pathology in mice. *Iscience*. 2022;25(4):103964.
38. Horne JA, Östberg O. A self-assessment questionnaire to determine morningness-eveningness in human circadian rhythms. *International journal of chronobiology*. 1976.
39. Roenneberg T, Wirz-Justice A, Meroz M. Life between clocks: daily temporal patterns of human chronotypes. *Journal of biological rhythms*. 2003;18(1):80–90.
40. Carney CE, Buysse DJ, Ancoli-Israel S, Edinger JD, Krystal AD, Lichstein KL, et al. The consensus sleep diary: standardizing prospective sleep self-monitoring. *Sleep*. 2012;35(2):287–302.
41. Mallinson DC, Kamenetsky ME, Hagen EW, Peppard PE. Subjective sleep measurement: comparing sleep diary to questionnaire. *Nature and Science of Sleep*. 2019;11:197.
42. Khosla S, Deak MC, Gault D, Goldstein CA, Hwang D, Kwon Y, et al. Consumer sleep technology: an American Academy of Sleep Medicine position statement. *Journal of clinical sleep medicine*. 2018;14(5):877–880.
43. Chinoy ED, Cuellar JA, Huwa KE, Jameson JT, Watson CH, Bessman SC, et al. Performance of seven consumer sleep-tracking devices compared with polysomnography. *Sleep*. 2021;44(5):zsa291.
44. Haghayegh S, Khoshnevis S, Smolensky MH, Diller KR, Castriotta RJ, et al. Accuracy of wristband Fitbit models in assessing sleep: systematic review and meta-analysis. *Journal of medical Internet research*. 2019;21(11):e16273.
45. Montes J, Tandy R, Young J, Lee SP, Navalta JW. Step count reliability and validity of five wearable technology devices while walking and jogging in both a free motion setting and on a treadmill. *International Journal of Exercise Science*. 2020;13(7):410.
46. Chevance G, Baretta D, Romain AJ, Godino JG, Bernard P. Day-to-day associations between sleep and physical activity: a set of person-specific analyses in adults with overweight and obesity. *Journal of Behavioral Medicine*. 2022;45(1):14–27.

47. Rosenbaum PR, Rubin DB. The central role of the propensity score in observational studies for causal effects. *Biometrika*. 1983;70(1):41–55.
48. Greenland S, Robins JM, Pearl J. Confounding and collapsibility in causal inference. *Statistical science*. 1999;29–46.
49. Greenland S, Robins JM. Identifiability, exchangeability and confounding revisited. *Epidemiologic Perspectives & Innovations*. 2009;6(1):4.
50. Rubin DB. Randomization analysis of experimental data: The Fisher randomization test comment. *Journal of the American statistical association*. 1980;75(371):591–593.
51. Cox DR. Planning of experiments. ” ”. 1958.
52. Rubin DB. Comment: Neyman (1923) and causal inference in experiments and observational studies. *Statistical Science*. 1990;5(4):472–480.
53. Hudgens MG, Halloran ME. Toward causal inference with interference. *Journal of the American Statistical Association*. 2008;103(482):832–842.
54. Dawid AP. Influence diagrams for causal modelling and inference. *International Statistical Review*. 2002;70(2):161–189.
55. Dawid AP, Didelez V. Identifying the consequences of dynamic treatment strategies. *Research Report*; 2005.
56. Dawid AP, Didelez V. Identifying the consequences of dynamic treatment strategies: A decision-theoretic overview. *Statistics Surveys*. 2010;4:184–231.
57. Eichler M. Causal inference in time series analysis. *Causality: Statistical Perspectives and Applications*. 2012:327–354.
58. Bühlmann P. Invariance, causality and robustness. *Statistical Science*. 2020;35(3):404–426.
59. Neto EC, Prentice RL, Bot BM, Kellen M, Friend SH, Trister AD, et al. Towards personalized causal inference of medication response in mobile health: an instrumental variable approach for randomized trials with imperfect compliance. *arXiv preprint arXiv:160401055*. 2016.
60. Neto EC, Perumal TM, Pratap A, Bot BM, Mangravite L, Omberg L. On the analysis of personalized medication response and classification of case vs control patients in mobile health studies: the mPower case study. *arXiv preprint arXiv:170609574*. 2017.
61. Hayashi F. *Econometrics*. Princeton University Press; 2000.
62. Aronow PM, Samii C. Estimating average causal effects under interference between units. *arXiv preprint arXiv:13056156*. 2013;3(4):16.
63. Sävje F, Aronow PM, Hudgens MG. Average treatment effects in the presence of unknown interference. *The Annals of Statistics*. 2021;49(2):673–701.
64. Robins J. A new approach to causal inference in mortality studies with a sustained exposure period—application to control of the healthy worker survivor effect. *Mathematical Modelling*. 1986;7(9-12):1393–1512.
65. Pearl J, Robins J. Probabilistic evaluation of sequential plans from causal models with hidden variables. In: *Proceedings of the Eleventh Conference on Uncertainty in Artificial Intelligence*. Morgan Kaufmann Publishers Inc.; 1995. p. 444–453.
66. Lunceford JK, Davidian M. Stratification and weighting via the propensity score in estimation of causal treatment effects: A comparative study. *Statistics in Medicine*. 2004;23(19):2937–2960.

67. Hernán MA, Robins JM. Estimating causal effects from epidemiological data. *Journal of Epidemiology and Community Health*. 2006;60(7):578–586.
68. Robins JM, Hernán MA. Estimation of the causal effects of time-varying exposures. *Longitudinal Data Analysis*. 2009:553–599.
69. Pearl J. *Causality*. 2nd ed. Cambridge University Press, USA; 2009.
70. Morgan SL, Winship C. *Counterfactuals and Causal Inference*. Cambridge University Press; 2014.
71. Hirano K, Imbens GW. Estimation of causal effects using propensity score weighting: An application to data on right heart catheterization. *Health Services and Outcomes research methodology*. 2001;2(3):259–278.
72. Horvitz DG, Thompson DJ. A generalization of sampling without replacement from a finite universe. *Journal of the American Statistical Association*. 1952;47(260):663–685.
73. Robins JM. Marginal structural models. 1997 Proceedings of the section on Bayesian statistical science. 1997:1–10.
74. Bang H, Robins JM. Doubly robust estimation in missing data and causal inference models. *Biometrics*. 2005;61(4):962–973.
75. Arlot S, Celisse A. A survey of cross-validation procedures for model selection. *Statistics surveys*. 2010;4:40–79.
76. Yang Y. Consistency of cross validation for comparing regression procedures. *The Annals of Statistics*. 2007;35(6):2450–2473.
77. Athey S, Imbens GW. Machine learning methods for estimating heterogeneous causal effects. arXiv:150401132v1 [statML] 5 Apr 2015. 2015:1–24.
78. Robins JM, Hernan MA, Brumback B. Marginal structural models and causal inference in epidemiology. *Epidemiology*. 2000;11:550–560.
79. Malenica I, Bibaut A, van der Laan MJ. Adaptive Sequential Design for a Single Time-Series. arXiv preprint arXiv:210200102. 2021.
80. Moraffah R, Sheth P, Karami M, Bhattacharya A, Wang Q, Tahir A, et al. Causal inference for time series analysis: Problems, methods and evaluation. *Knowledge and Information Systems*. 2021:1–45.
81. Daza EJ. Person as Population: A Longitudinal View of Single-Subject Causal Inference for Analyzing Self-Tracked Health Data. arXiv preprint arXiv:190103423. 2019.
82. Daza EJ, Wac K, Oppedo M; MDPI. Effects of sleep deprivation on blood glucose, food cravings, and affect in a non-diabetic: an N-of-1 randomized pilot study. *Healthcare*. 2019;8(1):6.
83. Goldsmith J, Zipunnikov V, Schrack J. Generalized multilevel function-on-scalar regression and principal component analysis. *Biometrics*. 2015;71(2):344–353.
84. Pearl J. Causal diagrams for empirical research. *Biometrika*. 1995;82(4):669–688.
85. VanderWeele TJ, Robins JM. Directed acyclic graphs, sufficient causes, and the properties of conditioning on a common effect. *American Journal of Epidemiology*. 2007;166(9):1096–1104.
86. Zucker D, Schmid C, McIntosh M, D’Agostino R, Selker H, Lau J. Combining single patient (N-of-1) trials to estimate population treatment effects and to evaluate individual patient responses to treatment. *Journal of Clinical Epidemiology*. 1997;50(4):401–410.
87. Zucker DR, Ruthazer R, Schmid CH. Individual (N-of-1) trials can be combined to give population comparative treatment effect estimates: methodologic considerations. *Journal of clinical epidemiology*. 2010;63(12):1312–1323.

A comprehensive list of references on statistical methods for within-individual studies can be found at <https://statsof1.org/resources/>.

Appendix for “MoTR and PSTn: Building a Causal Engine for Estimating the Within-Individual Average Treatment Effect Using Wearable Sensors”

Eric J. Daza, DrPH, MPS and Logan Schneider, MD

August 3, 2022

The following material is organized by relevant section numbers found in the main manuscript.

1 Introduction

1.1 Within-Individual Studies

Relationship to Hierarchical Models and Bayesian Inference

Analytically, the paradigm shift from hierarchical to within-individual studies is made precise at the level of inference and in the population’s temporal properties. The key estimand of a hierarchical study is a *group-level average* across a *contemporaneous* population, where autocorrelation induced by repeated measurements is a “nuisance” to conducting inference properly (often involving nuisance parameters). The key estimand of a within-individual study is an *individual-level average* across a *sequential* population; the nature of any autocorrelation may sometimes itself be of interest (e.g., as an effect modifier or moderator).

In data-processing terms, one can think of a table individuals as rows and sequentially recurring outcomes per individual as columns. The shift in focus would be from “long to wide”.

A Bayesian approach might involve using one’s personal beliefs and history to elicit the prior distribution of person-specific ARCO parameters. The epistemological focus of a within-individual study is on one person—at a time, at least. Hence, it is reasonable to primarily (if not wholly) rely on that particular individual’s experiences in constructing a priori hypotheses when feasible. Consideration or analysis of previously collected self-tracked (i.e., collected on oneself) data can help refine these hypotheses, as can group-level scientific findings (e.g., the latter might be used to set starting values for computationally iterative approaches).

2 Methodological Theory

2.9 ARCO in an N-of-1 Experiment

Here is the derivation of the long-run mean outcome for the ARCO model of order 1 specified in the text.

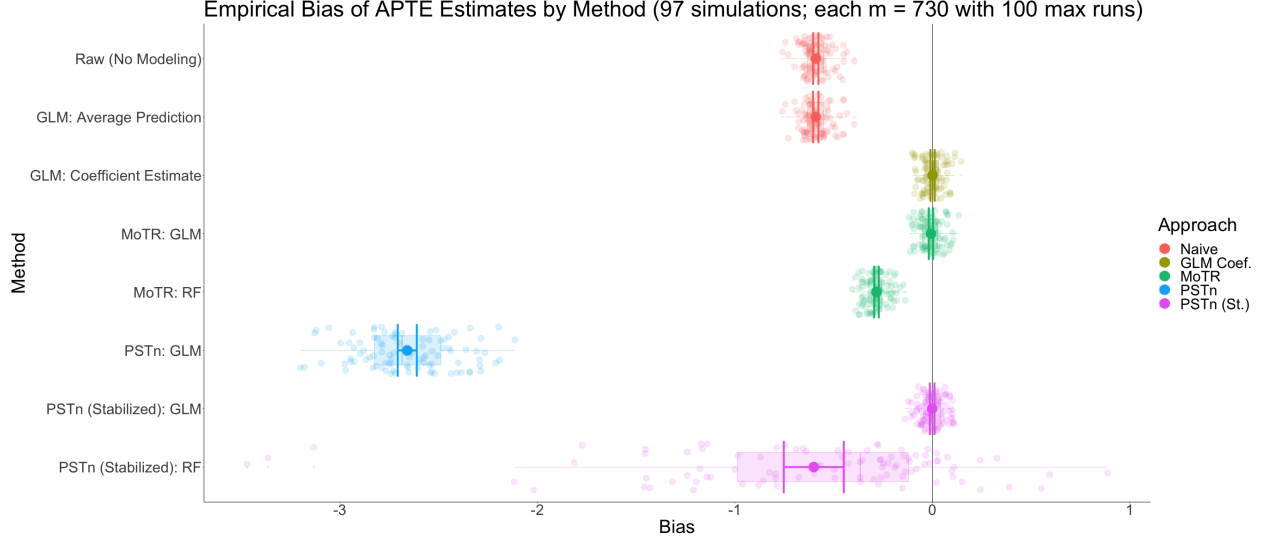


Figure A1: Analysis results of applying each method to 100 synthetic datasets with $m = 730$. Each light dot represents the empirical bias of one synthetic dataset for estimating a true APTE of 1.1. Each dark dot represents the average empirical bias over all 100 datasets, with corresponding 95% confidence interval shown as symmetric error bars.

$$\begin{aligned}
\mu_Y &= E(Y_t) \\
&= E(Y_t|X_t = 1)\pi + E(Y_t|X_t = 0)(1 - \pi) \\
&= (\alpha + \delta^{\text{APTE}})\pi + \alpha(1 - \pi) \\
&= \alpha\pi + \delta^{\text{APTE}}\pi + \alpha - \alpha\pi \\
&= \delta^{\text{APTE}}\pi + \alpha \\
&= (\beta_X + \beta_{X_{co}}\pi + \beta_{X_{ar}}\mu_Y)\pi + \beta_0 + \beta_{co}\pi + \beta_{ar}\mu_Y + \boldsymbol{\mu}_V\boldsymbol{\beta}_{ex} \\
&= \beta_X\pi + \beta_{X_{co}}\pi^2 + \beta_{X_{ar}}\mu_Y\pi + \beta_0 + \beta_{co}\pi + \beta_{ar}\mu_Y + \boldsymbol{\mu}_V\boldsymbol{\beta}_{ex} \\
\mu_Y - \beta_{X_{ar}}\mu_Y\pi - \beta_{ar}\mu_Y &= \beta_X\pi + \beta_{X_{co}}\pi^2 + \beta_0 + \beta_{co}\pi + \boldsymbol{\mu}_V\boldsymbol{\beta}_{ex} \\
\mu_Y - \beta_{ar}\mu_Y - \beta_{X_{ar}}\mu_Y\pi &= \beta_0 + \beta_X\pi + \beta_{co}\pi + \beta_{X_{co}}\pi^2 + \boldsymbol{\mu}_V\boldsymbol{\beta}_{ex} \\
\mu_Y(1 - \beta_{ar} - \beta_{X_{ar}}\pi) &= \beta_0 + \beta_X\pi + \beta_{co}\pi + \beta_{X_{co}}\pi^2 + \boldsymbol{\mu}_V\boldsymbol{\beta}_{ex} \\
\mu_Y &= \frac{\beta_0 + \beta_X\pi + \beta_{co}\pi + \beta_{X_{co}}\pi^2 + \boldsymbol{\mu}_V\boldsymbol{\beta}_{ex}}{1 - \beta_{ar} - \beta_{X_{ar}}\pi}
\end{aligned}$$

4 Simulation Study

4.2 Analysis Methods and Results

5 Empirical Study

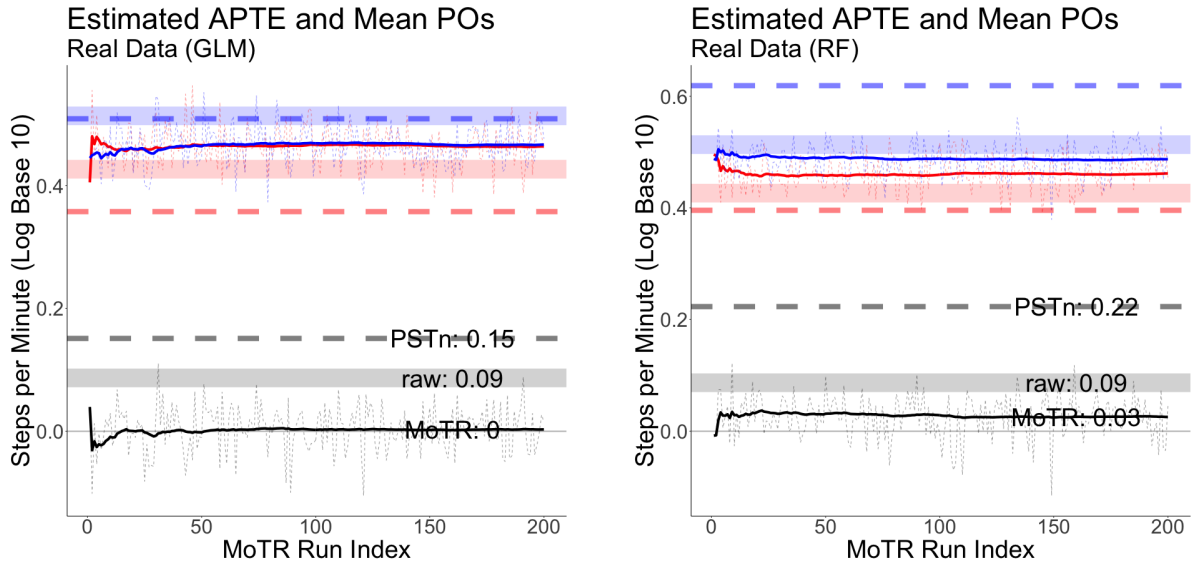


Figure A2: Analysis results of applying each method to real dataset; i.e., generalized linear model (GLM) or random forests (RF). MoTR used $r_{min} = 10$ to $r_{max} = 200$ runs. The legend is identical to that in the Figure 1 caption.